# SUBJECT-SPECIFIC FINITE ELEMENT MODELING OF THE TIBIOFEMORAL JOINT *IN VIVO*: DEVELOPMENT, VERIFICATION AND APPLICATION

by

**Robert Edward Carey**

B.S. in Mechanical Engineering, University of Pittsburgh, 2011

Submitted to the Graduate Faculty of

Swanson School of Engineering in partial fulfillment

of the requirements for the degree of

M.S. in Mechanical Engineering

University of Pittsburgh

2014

UNIVERSITY OF PITTSBURGH

SWANSON SCHOOL OF ENGINEERING

This thesis was presented

by

Robert Edward Carey

It was defended on

March 25, 2014

and approved by

Jeffrey S. Vipperman, PhD, Associate Professor

Patrick Smolinski, PhD, Associate Professor

Mark C. Miller, PhD, Associate Research Professor

Thesis Advisor: Xudong Zhang, PhD, Associate Professor

**SUBJECT-SPECIFIC FINITE ELEMENT MODELING OF THE TIBIOFEMORAL JOINT *IN VIVO*: DEVELOPMENT, VERIFICATION AND APPLICATION**

Robert Edward Carey, M.S.

University of Pittsburgh, 2014

A new methodology for subject-specific finite element (FE) modeling of the tibiofemoral (TF) joint based on *in vivo* computed tomography (CT), magnetic resonance imaging (MRI), and dynamic stereo-radiography (DSX) data is presented. Two techniques to incorporate *in vivo* skeletal kinematics as FE boundary conditions were implemented and compared: one used MRI-measured tibiofemoral kinematics in a non-weight-bearing supine position and allowed five degrees of freedom at the joint in response to an axially applied force; the other used DSX-measured tibiofemoral kinematics in a weight-bearing standing position and permitted only axial translation in response to the same force. The model-predicted cartilage-cartilage contact areas were examined against 'benchmarks' from a novel *in situ* contact area analysis (ISCAA) in which the intersection volume between non-deformed femoral and tibial cartilage was characterized to determine the contact. The results showed that the DSX-based model predicted contact areas in close alignment with the benchmarks, and outperformed the MRI-based model. The importance of accurate, task-specific skeletal kinematics in subject-specific FE modeling and the necessity of subject-specific verification are discussed.

A study of the effects of partial meniscectomy on the intra-articular contact mechanics was then conducted as an illustration of application of the verified models. A musculoskeletal dynamic model was used to generate the knee joint forces as boundary conditions for the above developed FE models. Thus, a sequence of quasi-static position-dependent FE models was

developed for a series of time points throughout a decline walking task. These time points include heel-strike and in increments of 0.05 seconds up to 0.30 seconds, and additionally, the time points of the two peak compressive joint force values for each knee. Several factors were observed to measure the effects on intra-articular contact mechanics. The greatest maximum compressive stress was recorded in the partially meniscectomized compartment or in the opposite compartment of the contralateral knee throughout all time points. The significance of the application of the FE models for evaluation of the biomechanical effects of meniscectomy is demonstrated, and the importance of simultaneously observing joint kinematics and intra-articular contact mechanics at more than one time point during a dynamic task is discussed.

## TABLE OF CONTENTS

## LIST OF TABLES

## LIST OF FIGURES

## PREFACE

I would like to first acknowledge the opportunity provided to me by the Almighty Lord, who has blessed me and guided me throughout my years and given me the strength and courage to be who I am today. I would also like to acknowledge the support and love given to me by my family, including my father Francis, my mother Kathleen and my older brother Matthew. Both my parents have graced me with their love throughout my life and have provided me with everything I have ever needed. Without them, I would not be where I am today. Through my brother, I have learned the traits of hard work and determination in order to achieve my goals, and have realized that I have the ability to accomplish anything.

I deeply thank my advisor Dr. Xudong Zhang, who saw potential in me and provided me the opportunity to continue my education and a chance to make a contribution to the field of biomechanics. He has given me his time, advice, criticism and guidance to see that I become a more productive member in the biomechanics research field.

I extend my thanks to Drs. Ameet Aiyangar and Liying Zheng for their help and guidance throughout my graduate career. Both have donated time and effort to lend guidance and aid in my research efforts, instilling their knowledge in the biomechanics field into my work. Without them, I would not have been able to accomplish all of the work presented in this thesis. Not only did they spend time with me professionally, but also on a personal level, which has deepened the bond between us.

I am appreciative to those in the mechanical engineering department at the University of Pittsburgh who provided me the opportunity to study within the school, including Drs. Jeffrey Vipperman, Minking Chyu and Qing-Ming Wang. To my Master's thesis defense committee, Drs. Vipperman, Patrick Smolinski and Mark Miller, I am grateful for the time taken out of their busy schedules and their insightful comments. I would like to acknowledge Dr. Scott Tashman for technical advice on dynamic stereo-radiography data acquisition, Dr. Christopher Harner for his clinical knowledge and insights and Mr. Eric Thorhauer and Dr. Snehal Shetye for their technical assistance throughout my research efforts. I also extend my gratitude towards the rest of the research family in the Sports Orthopaedic Research Lab and Musculoskeletal Modeling Lab for their support, especially Mrs. Julie Mathis.

I would like to acknowledge the generous support by the Musculoskeletal Transplant Foundation (MTF), NIH (R03-AR059939), and a University of Pittsburgh Department of Mechanical Engineering & Materials Science Graduate Tuition Scholarship.

# 1.0 BACKGROUND

## 1.1 MOTIVATION

The knee joint is a complex combination of hard tissues (such as bones) and soft tissue (such as menisci, ligaments and cartilage), allowing for locomotion of the body. Therefore, it is important to retain the overall health of the knee joint, including all components that compromise the joint.

Two of these components that are essential to joint function are the menisci and articular cartilage. The menisci are semi-lunar fibro-cartilaginous tissue that contains a solid phase and a fluid phase. The solid phase is composed primarily of collagen fibers, which provide a large tensile stiffness and strength and are arranged in different orientations for different functions (Figure 1) [1]. Mechanical function of the menisci is contingent not only upon its material makeup, but also its shape, the shapes of interaction components, and boundary conditions. The menisci sit upon the tibial articular cartilage, and are anchored in the tibial plateau at the anterior and posterior horns, which prevent displacement of the menisci when loads are applied to the knee. With their wedged shape, the menisci displace forces from the rounded femoral condyles and transfer these forces through the tibia via the flat tibial plateau and articular cartilage [1]. The role of the menisci is to aid in stability, proprioception, lubrication, shock absorption and load distribution [2]. The latter function is a key responsibility in maintaining joint congruency,

and disruption of the menisci, such as removal due to meniscectomy (Figure 2), can cause changes that may alter the intra-articular contact mechanics of the TF joint, resulting in damage to the surrounding soft tissue, such as articular cartilage.

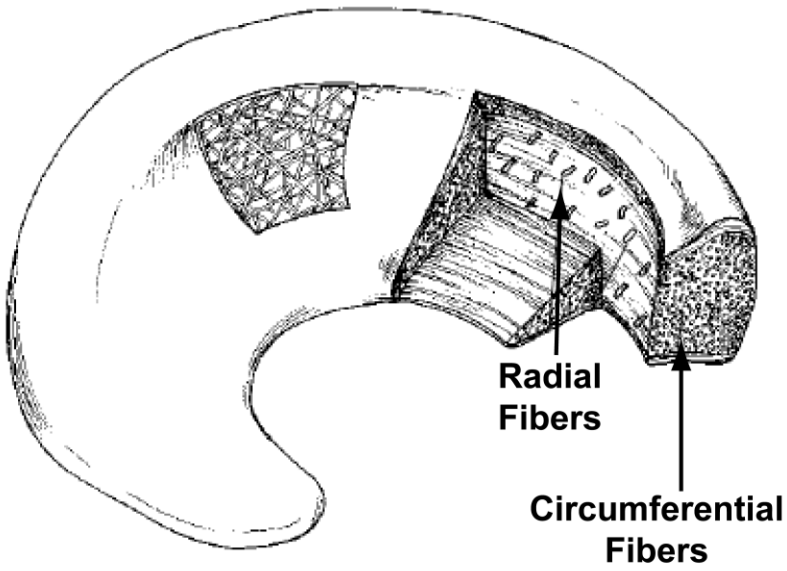


Figure 1: Image of a meniscus showing the radial and circumferential collagen fiber orientation [3].

Another component essential to joint function is the articular cartilage, a hyaline cartilage covering of the subchondral bone on both the femur and tibia of the tibiofemoral (TF) complex. Articular cartilage consists primarily of collagen, which provides a large tensile property to the cartilage at the articulating surface, allowing for the ability to accommodate large shear, tensile and compressive stresses. The articulating surface retains special molecules called superficial zone proteins, which play an important role in the nearly frictionless surfaces of the articular cartilage, and in combination with the joint synovial fluid, allows for ease of joint articulation [4]. Damage to the articular cartilage, such as fibrillation of the articulating surface, can reduce

the ease of joint articulation, and can lead to osteoarthritis (OA), a painful and debilitating disease [5].

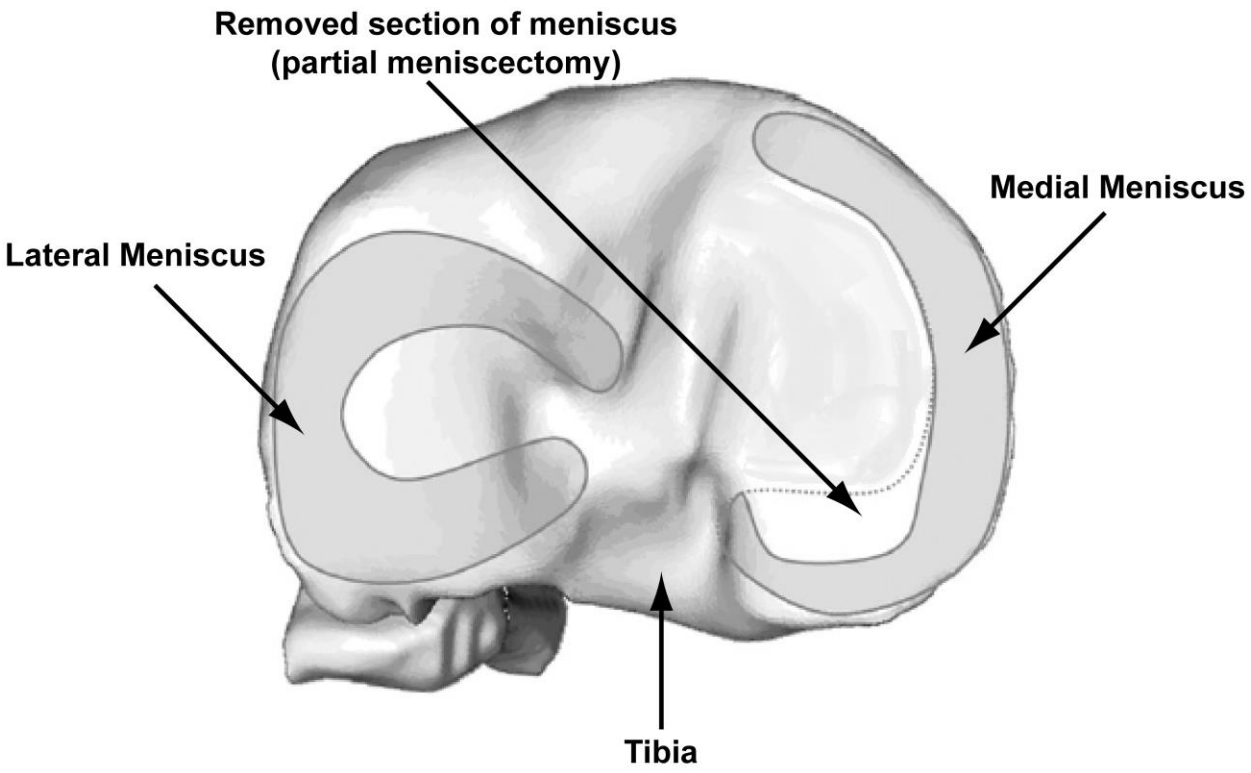


Figure 2: Image showing the area of a meniscus removed in a partial meniscectomy [6].

OA, considered to be a major worldwide cause of economic loss, is the most common degenerative joint disease. It is usually diagnosed through radiographic evidence of articular cartilage loss, osteophytes, an increased subchondral bone density and cysts. More than 1/3 of all people over the age of 45 report joint symptoms consistent with OA, including loss of motion and constant deep pain. The World Health Organization estimates that 10% of the world's population aged 60 and up suffer from OA. Of these individuals, it is believed that 80% have limited movement and that 25% cannot perform standard daily activities [5]. Once an individual develops OA, he or she suffers from the disease the rest of his or her life, and the severity of the

symptoms, such as the pain, only increases with time. Solving the issue of OA will require a method of either stunting the progression of joint degeneration, such as articular cartilage damage and loss, or developing a way to prevent it entirely [5].

Injury of the meniscus is one of the most common knee injuries, with as many as one million meniscal procedures performed annually in the United States [7, 8]. Of these procedures, meniscectomy is one of the most popular surgical options to relieve pain caused by the injury [9]. It has been observed that those with injuries of TF joint components have an accelerated onset of OA [10-19]. Thus, it is imperative that the relationships between injury/treatment, changes in intra-articular contact mechanics and the accelerated onset of OA be better understood so that a solution can be found for the prevention of OA (Figure 3).

It has been shown that disruption of the meniscus, such as removal by meniscectomy, can lead to degenerative changes of the TF articular cartilage, preceding OA [1, 20, 21]. This has been established through clinical observations (Figure 3b). It has also been seen that changes in the TF intra-articular contact mechanics due to injury or treatment are linked to accelerated loss of cartilage, also leading to the early beginning of OA (Figure 3c). Andriacchi et al. [22] utilized a cartilage defect algorithm in conjunction with a FE model in order to simulate the effect of increased stress on the thinning of the TF articular cartilage. The work presented below will focus on the third link of this relationship: how injury or treatment of a TF joint component can cause changes in the intra-articular contact mechanics (Figure 3a).

There are different computational methods for the study of TF intra-articular contact mechanics. Two popular methods are discrete element analysis (DEA) and finite element analysis (FEA). DEA is a method in which contact forces between two bodies are modeled using a spring-damper relationship. This simplification allows for computationally efficient

models to be developed, even with complex geometries. FEA uses the calculus of variations, alongside the deformation of solid mechanics, and attempts to minimize an error function to produce a stable solution. FEA is not as computationally efficient as DEA for small scale models, but tends to produces more accurate predictions. Abraham et al. compared a validated FEA model to a DEA model of the hip joint, and found that the DEA model produced only general trends for contact stress magnitudes, but failed to reliably predict the true magnitude [23]. Thus, for more accurate predictions of intra-articular contact mechanics, FEA was chosen for these studies.

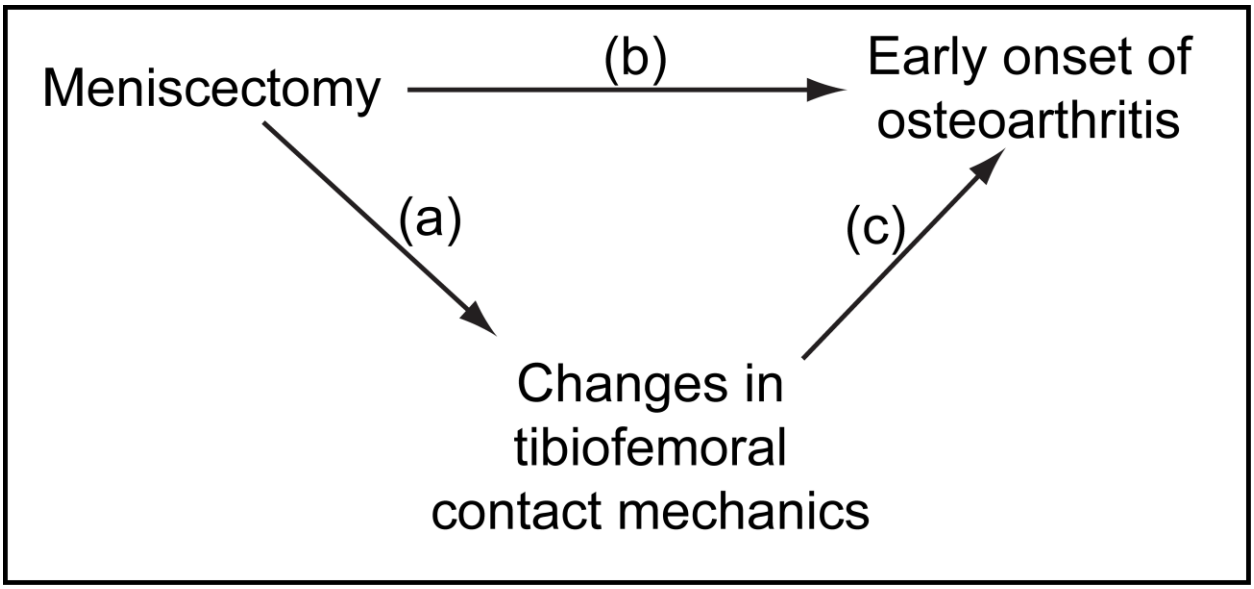


Figure 3: Three important relationships for the understanding and prevention of early OA onset: (a) the relationship between meniscectomy and changes in tibiofemoral contact mechanics, (b) the relationship between meniscectomy and the early onset of osteoarthritis and (c) the relationship between changes in tibiofemoral contact mechanics and the early onset of osteoarthritis.

Finite element (FE) modeling provides a useful technique that can be applied to the study of OA prevention. A relative new computational modeling process, it allows for the

approximated solution to simple and complex boundary value problems by using approximation to the mathematical components behind three-dimensional solid mechanics. FE modeling has been used for the study of biological tissue on a microscopic level [24], a macroscopic level [25], prosthetic devices [26], fracture mechanics [27] and insight into pathology [28]. Although FE modeling comes with a high computational cost, developments in technology will further allow for the increase in speed of simulations and for the increased complexity of the model being simulated, which can lead to more accurate representations of biological features and better insights into their mechanical responses.

## 1.2 SUMMARY

The goals of this thesis are to develop subject- and task-specific FE models using highly accurate geometry, kinematics and kinetics, verify the subsequent models using a novel subject- and task-specific technique, and apply these models to study the effects of partial meniscectomy on the intra-articular contact mechanics.

The models will be developed using an integrative multi-modality approach, utilizing computed tomography, magnetic resonance imaging and dynamic stereo-radiography data. Two methods to incorporate kinematics into the models will be used and verified by an *in situ* contact area analysis developed to compare cartilage-to-cartilage contact centroids on the tibial cartilage. The material properties chosen for the models will be subject to a sensitivity analysis to determine their overall effect on the verification process.

Once the verified models are created, they will be applied to study a decline walking task of a subject with a partial meniscectomy in the lateral compartment of the left knee and a healthy contralateral knee. Subject- and task-specific kinetics will be developed through the use of dynamic stereo-radiography, skin surface markers and ground reaction forces using a musculoskeletal dynamic model. From this model, knee joint compressive forces will be extracted and applied to the models, along with corresponding kinematics to complete the modeling task. Intra-articular contact mechanics, such as cartilage-to-cartilage contact area and maximum compressive stress will be compared between the partially meniscectomized knee and the healthy knee.

In Chapter 2, the model development and verification process will be discussed, including the methods used to turn multi-modality data into subject-specific FE models and the novel technique for verifying the models using subject-specific data.

# 2.0 DEVELOPMENT AND VERIFICATION

## 2.1 INTRODUCTION

Finite element (FE) modeling is a powerful tool for studying joint and tissue mechanics, as it enables manipulation of variables and simulation of situations that may be challenging or infeasible to evaluate clinically or experimentally. The accuracy of FE model solutions depends on well-defined anatomical geometry, material properties and boundary conditions [29]. Given the considerable inter-subject variability in tissue structure morphology, personalized analyses and insights would require subject-specific FE modeling [30]. *In vivo* FE modeling efforts have been limited by difficulties in acquiring and analyzing multi-modality data for model construction and validation, including proper co-registration and integration of all necessary data. Recent advances in the fields of medical imaging and image reconstruction have increased the potential to incorporate accurate tissue morphology and boundary conditions into *in vivo* subject-specific models [31].

Nevertheless, the veracity of FE model predictions hinges upon at least two challenging aspects: accurate representation of joint kinematics during functional tasks, and validation or verification of the model with experimentally measurable parameters obtained *in vivo*. Previous *in vivo* TF FE modeling efforts have created models without sufficiently considering the

functional joint kinematics involved in the joint loading process [32, 33]. Studies have incorporated skeletal kinematics from either non-subject-specific data [22, 34, 35] or skin surface marker measurements [36, 37]—the latter are prone to soft-tissue artifacts [38] due to marker movement [39, 40] and inaccurate marker positioning on the skin relative to the bone [41, 42]. Two FE studies have employed advanced imaging techniques to acquire skeletal kinematics: Beillas et al. [34, 35] used X-ray imaging that required surgical implantation of radio-opaque markers into the bone; Yao et al. [43] utilized a loading device to exert a force on the knee as it was undergoing magnetic resonance imaging (MRI) in a supine position. While these studies were successful attempts to incorporate task-specific [34, 35] or load-specific [43] kinematics, quantitative verification of their FE model predictions was not conducted. Validation or verification is a crucial step before making interpretations based on model predictions or using the model for clinical applications [21, 44]. Conventional measures for FE model validation, such as contact pressure [31], cannot be reliably acquired without invasive procedures and are not applicable to *in vivo* subject-specific models. However, it is possible to estimate the contact area and centroid *in vivo* without invasive procedures with a technique we present here.

This study was motivated by the need for a validated subject-specific FE modeling methodology to study joint mechanics and functions in response to various musculoskeletal injuries and their treatments. While it is believed that the methodology can be generalized to other articulating joint structures, this study focused on the TF joint, meniscus injury and meniscectomy. The meniscus is an integral component of the knee, playing a vital role in stability, proprioception, lubrication and load distribution [2, 10, 17, 45]. It has been shown that meniscectomy, a common treatment for meniscal injuries and one of the most frequently performed orthopaedic procedures, can lead to degenerative changes of the articular cartilage in

the knee [17, 20, 21, 46-48]. In order to better understand the relationship between meniscectomy and the onset as well as progression of articular cartilage damage, it is important to first assess the joint and tissue mechanical changes involved — a problem well suited for investigation based on FE modeling.

Specifically, we aimed to explore subject-specific FE modeling of the TF joint based on *in vivo* measurements of tissue morphology from high-resolution MRI and three-dimensional (3D) skeletal kinematics from dynamic stereo-radiography (DSX). This latter technology provides an ability to measure skeletal kinematics during functional tasks with sub-millimeter accuracy [49]. We proposed a novel *in situ* contact area analysis (ISCAA) technique, allowing the use of a subject's own data to validate the subject-specific FE model.

## 2.2 METHODS

The knee morphological and kinematic data for FE modeling were from an IRB-approved meniscus allograft transplantation experimental study. We used the data of one subject (female, age 19) who had previously undergone an arthroscopic partial meniscectomy of the lateral meniscus in the left leg. Data for both the meniscectomized left knee and intact right knee, collected prior to the transplantation surgery, were used. An overview of how multi-modality data (DSX, CT, and MRI) were acquired and integrated for model creation and verification is presented in Figure 4. The individual procedures from data acquisition to model verification are described as follows.

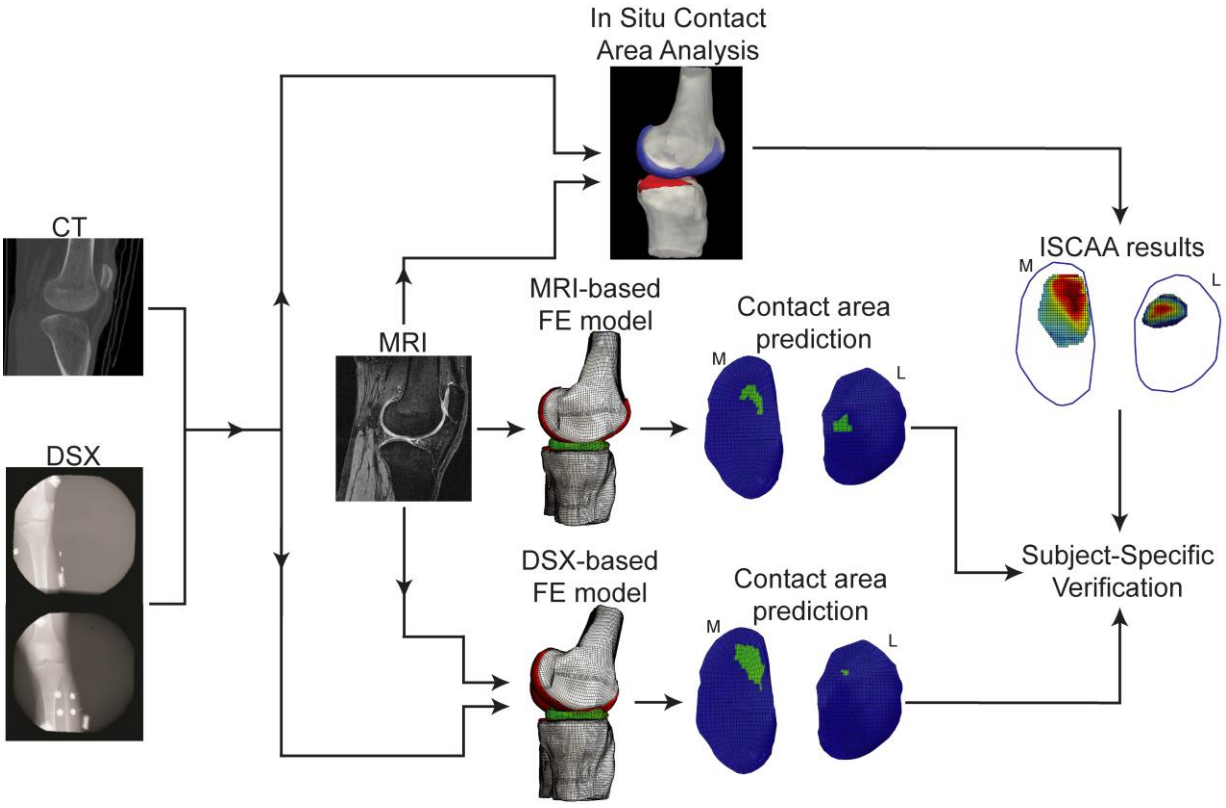


Figure 4: A flow chart of the FE model development and verification process incorporating multi-modality data.

### 2.2.1 Data Acquisition

The experimental setup consisted of a high-speed biplane radiographic system (Figure 5) for collecting X-ray images of the knee joint with the ability to capture dynamic skeletal kinematics within 0.2 mm and 0.2° [49]. Two high speed 4 mega pixel Phantom v10 cameras (Vision Research, New Jersey, USA) capable of capturing 250 images per second, each coupled with a 16-inch Thalus image intensifier (Shimadzu Medical Systems, Kyoto, Japan), a CPX-3100CV cardiac-cine angiography generator (EMD Technologies, Saint-Eustache, Canada) and a 0.3/0.6 mm focal spot X-ray tube were used to capture the TF skeletal kinematics.

The cardiac-cine generators were optimized to 80 kVp and 100 mA with an exposure pulse width of 1 ms in order to clearly capture the bone motion while minimizing radiation exposure to the subject, and were offset from each other by approximately 45° in order to fully acquire the 3D positions. The location of the cameras was also chosen in order to maximize the time that the desired knee was within the imaging volume and minimize the time of interference from the contralateral knee during movement. Kinematical data was captured while the subject performed the desired task on an instrumented dual belt treadmill (Bertec Corp., Columbus, Ohio, USA), which has the ability to record 3D ground-reaction forces for each half of the treadmill independently.

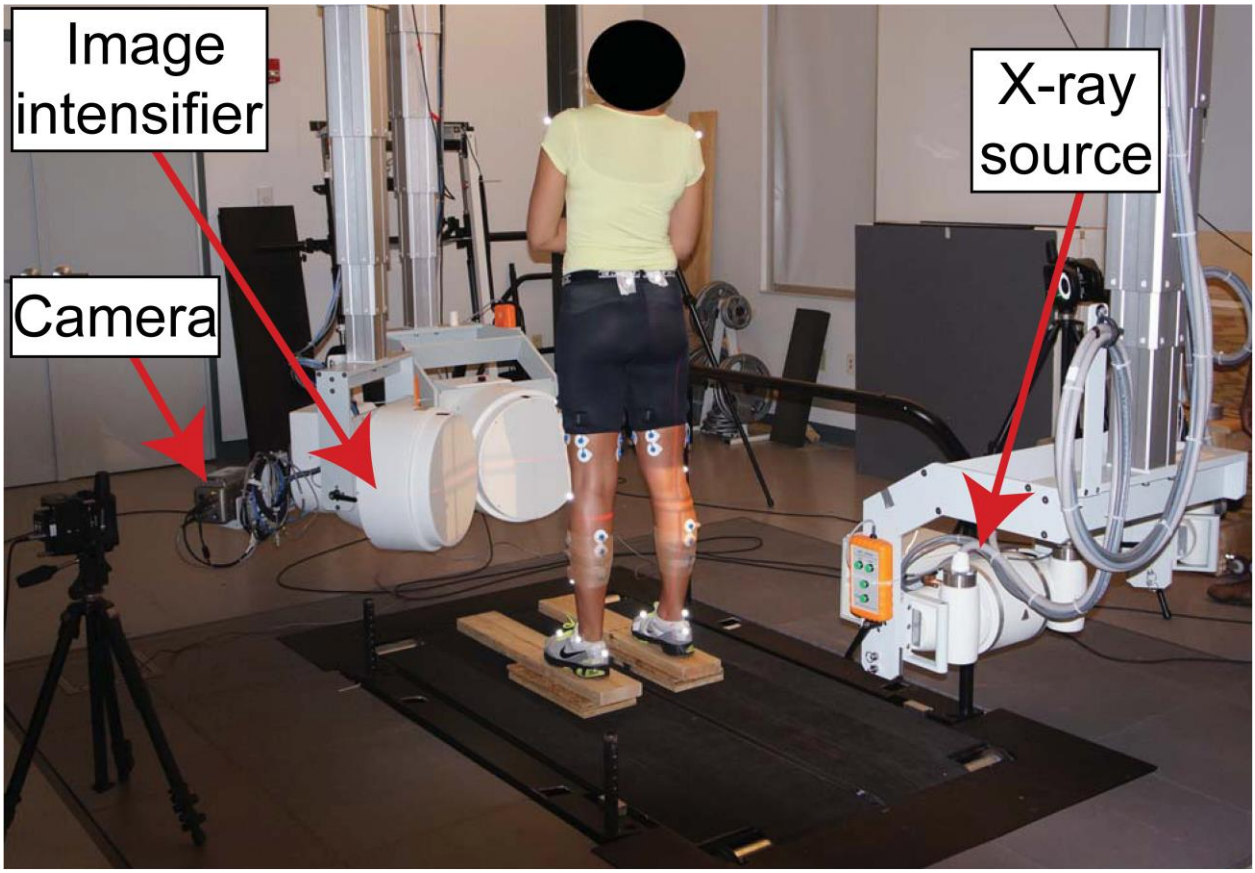


Figure 5: Experimental setup for measuring 3D TF skeletal kinematics during static standing using a dynamic stereo-radiography system.

A bilateral computed tomography (CT) scan (GE Medical Systems Lightspeed Pro 16, Waukesha, WI) of the subject's knees was obtained with the following specifications: pixel size = 0.586x0.586 $mm^2$, slice thickness = 1.25 mm, pixel resolution = 512x512 pixels, field of view (FOV) = 30.0 cm, number of slices = 123, excitation voltage = 120 kV, current-time = 402.8 mAs. The CT data were imported into Mimics 14.0 (Materialise, Ann Arbor, MI, USA) and segmented slice-by-slice to create a 3D bone model for both the femur and tibia. A custom model-based tracking software program was used to create a virtual testing configuration replicating that of the actual physical DSX system. The 3D bone models produced from CT were placed within the virtual environment to, through a ray-tracing algorithm, create digitally reconstructed radiographs (DRRs). A volumetric image-matching algorithm was then employed in a co-registration process between the DRRs and DSX images, optimizing the 3D position of the DRRs relative to the corresponding bone in the DSX images for each frame. Additional details on this model-based tracking technique can be found in a previous publication [50].

An MRI scan (Siemens Trio 3.0 Tesla, Washington, DC) of the knee joint was acquired while the subject was in a non-weight-bearing, supine position using a sagittal 3D dual echo steady state water excitation (DESS-WE) sequence. The MRI scan specifications were: pixel size = 0.365x0.365 $mm^2$, slice thickness = 0.7 mm, pixel resolution = 384x384 pixels, FOV = 14.0 cm, number of slices = 160.

### 2.2.2 Model Geometry

The MRI data were imported into Mimics 14.0 for creation of 3D models of the femur, tibia, femoral cartilage, tibial cartilage, and menisci. Once the 3D models were created, they were

imported into TrueGrid (XYZ Scientific, CA, USA) for manual linear hexahedral meshing. Each component was meshed separately and then imported into Abaqus CAE 6.9 (Simulia, RI, USA), where they were combined into a single FE model for an implicit analysis. Figure 6 shows an example of the FE model geometry development process. The numbers of elements in the FE models of individual components in each knee are listed in Table 1.

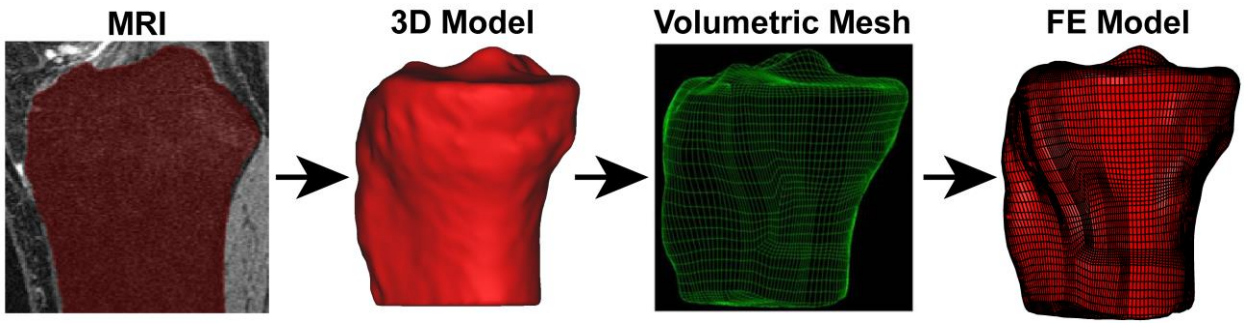


Figure 6: FE model geometry development sequence for the tibia.

### 2.2.3 Material Properties

Tissue material properties were taken from literature. The femur and tibia were modeled as rigid structures, which greatly reduced the computational time and has been shown to have minimal effect on the model predictions [22, 29, 32, 36, 46, 51-61]. Articular cartilage is known to be an anisotropic, biphasic material with a time constant approaching 1500 seconds [62, 63]. The compressive loading in this study was quasi-static. It has been shown that under this condition, the biphasic response of cartilage can be negligible and the single-phase linear isotropic constitutive law is applicable [62, 63]. Therefore, cartilage was modeled as a homogeneous,

elastic, linearly isotropic material [22, 29, 30, 32-34, 36, 43, 46, 47, 52, 54, 55, 57-61, 64-68] with a modulus of 15 MPa [32, 36, 47, 52, 57, 67] and a Poisson's ratio of 0.46 [53-55, 69, 70].

Table 1: Numbers of linear hexahedral elements in individual model components

| | *Meniscectomized Knee* | *Healthy Knee* |
|---|---|---|
| Femur | 41,984 | 76,308 |
| Tibia | 61,440 | 87,852 |
| Femoral Cartilage | 5,632 | 3,648 |
| Tibial Cartilage | 11,264 | 2,816 |
| Lateral Meniscus | 16,896 | 2,352 |
| Medial Meniscus | 16,896 | 2,112 |
| **Total** | 154,112 | 175,088 |

For the menisci, a transversely isotropic constitutive law was used in order to emphasize the dominant role played by the circumferential fibers in load distribution and function [1, 2, 10, 14, 71]. The menisci were therefore modeled as linearly elastic, transversely isotropic materials [29, 30, 32, 36, 37, 43, 47, 52, 56-58, 61, 65-67, 72], where the modulus and Poisson's ratio were 20 MPa and 0.2, respectively, in the radial and axial directions, and 140 MPa and 0.3, respectively, in the circumferential direction [32, 52, 67, 72]. Time dependent effects of the cartilage and menisci properties were not considered due to the quasi-static nature of the models [32, 34, 35, 46, 52, 54, 57, 62-64, 70, 73, 74]. The anterior and posterior meniscal roots for each

meniscus were modeled as linear springs with spring constants of 2000 N/mm [36, 46, 47, 52, 57, 58, 67, 72].

### 2.2.4 Kinematics and Loading Conditions

Two FE models were created for each knee, one incorporating MRI-based static supine kinematics and the other DSX-based static standing kinematics (Figure 7). The first FE model developed for each knee was based on the MRI data using the procedure described above, resulting in a model in the supine MRI position. In order to incorporate the static standing DSX-based kinematics, the DSX-acquired kinematics had to be transformed into the MRI-based coordinate system. For both the femur and tibia, the CT-based 3D model was co-registered to the MRI-based 3D model using Geomagic Studio 10 (Geomagic, North Carolina, USA). A manual n-point registration was completed by choosing three landmark points on the surface of the CT 3D bone model and then choosing the same three points on the surface of the MRI 3D bone model. This was done to create a close initial estimate for an automatic global registration process. The automatic global registration process was then executed, minimizing the co-registration error between the two 3D models. The average (± SD) error in the co-registration process for the bones was 0.472 (± 0.305) mm. This procedure output a transformation matrix from the CT coordinate system to the MRI coordinate system (CT-MRI). One output of the model-based tracking process was a transformation matrix from the laboratory coordinate system to the CT coordinate system (lab-CT). The lab-CT and CT-MRI transformation matrices for each respective bone were combined to yield a transformation matrix from the laboratory coordinate system to the MRI coordinate system (lab-MRI). These transformations were then

applied to each knee's MRI-based supine position FE model to create a model in the DSX-based static standing position. The tibial side lab-MRI transformation was applied to the tibia, tibial cartilage and menisci, while the femoral side lab-MRI transformation was applied to the femur and femoral cartilage.

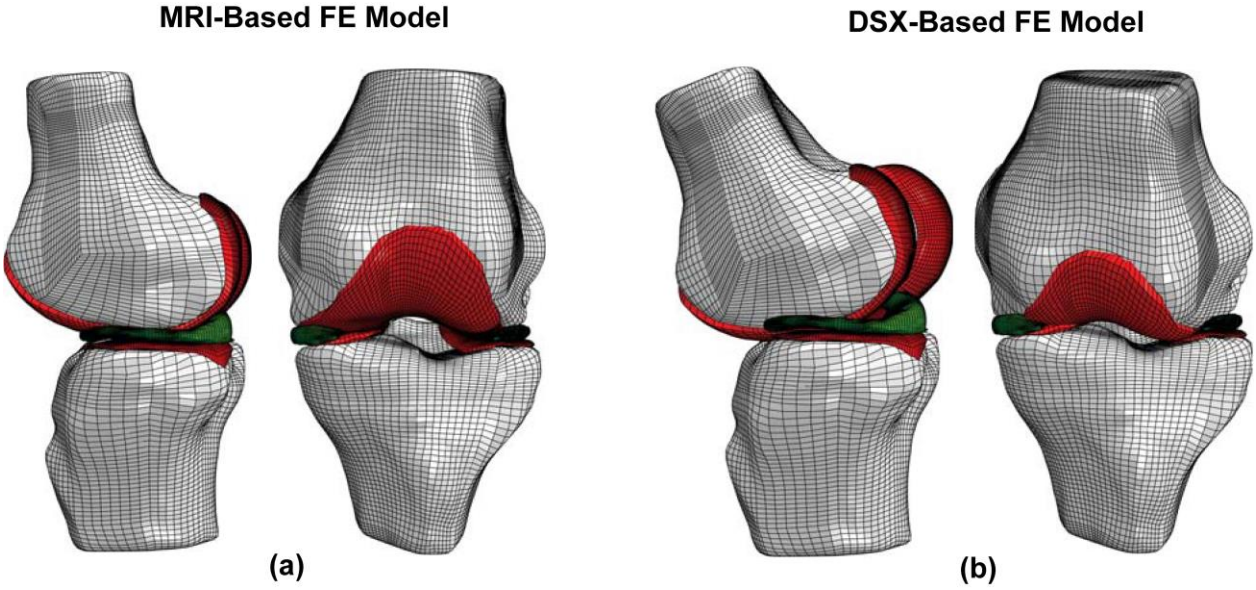


Figure 7: Lateral and anterior views of FE models of the meniscectomized knee in (a) MRI-based and (b) DSX-based positions.

For both the MRI-based and DSX-based models, the tibia was held in a fixed position while the femur was allowed to translate axially in response to a force of half the subject's body weight (275 N) applied to the proximal end of the femur towards the tibia. This force, along with contact pairs and prescribed boundary conditions, determined the "final position" of each model. For the model in the MRI-based supine position, five degrees of freedom (DOF) were allowed for the femur while the flexion-extension was fixed. For the model in the DSX-based

standing position, since the prescribed position of the femur relative to tibia is a final, known position from the experimental data, the only DOF permitted was an axial translation, allowing the femur to settle into its final position in response to the force applied. The femoral and tibial cartilage components were tied to the femur and tibia surfaces, respectively, while hard, frictionless contact was assumed for cartilage-cartilage and cartilage-meniscus interfaces [29, 32, 43, 46, 52, 54-57, 59-61, 64, 65, 67, 68, 70, 75]. In all models, a large-strain formulation was used [60, 68] to account for potentially substantial strains in the soft tissue components. The cartilage-to-cartilage contact area between the femoral and tibial cartilage from the resulting FE analysis was used as the measure for verification. The contact centroid was determined on the tibial cartilage for each compartment based on a transverse view of the superior cartilage surface.

### 2.2.5 Verification

An *in situ* contact area analysis (ISCAA) method was developed in order to verify the predictions of the FE models using cartilage-cartilage contact as the measure. The femoral and tibial cartilage in the DSX-based standing position was utilized. The cartilage surfaces in the MRI-based supine position were imported into Matlab 2012a (MathWorks, Massachusetts, USA). Cartilage was transformed into the DSX-based standing position by applying the lab-MRI transformation. The overlapped area between non-deformed femoral and tibial cartilage (Figure 8) was calculated and projected onto a single transverse plane determined as the least-squares-fit plane of the tibial cartilage, which provided a common reference for comparing the FE model-predicted and ISCAA-assessed contact centroids. The depth of overlap can be used as a surrogate measure of total cartilage strain [76]. The contact centroid for the ISCAA ($C_{ISCAA}$)

result was calculated and compared to the contact centroids obtained from the MRI-based supine position model ($C_{MRI}$) and the DSX-based standing position model ($C_{DSX}$).

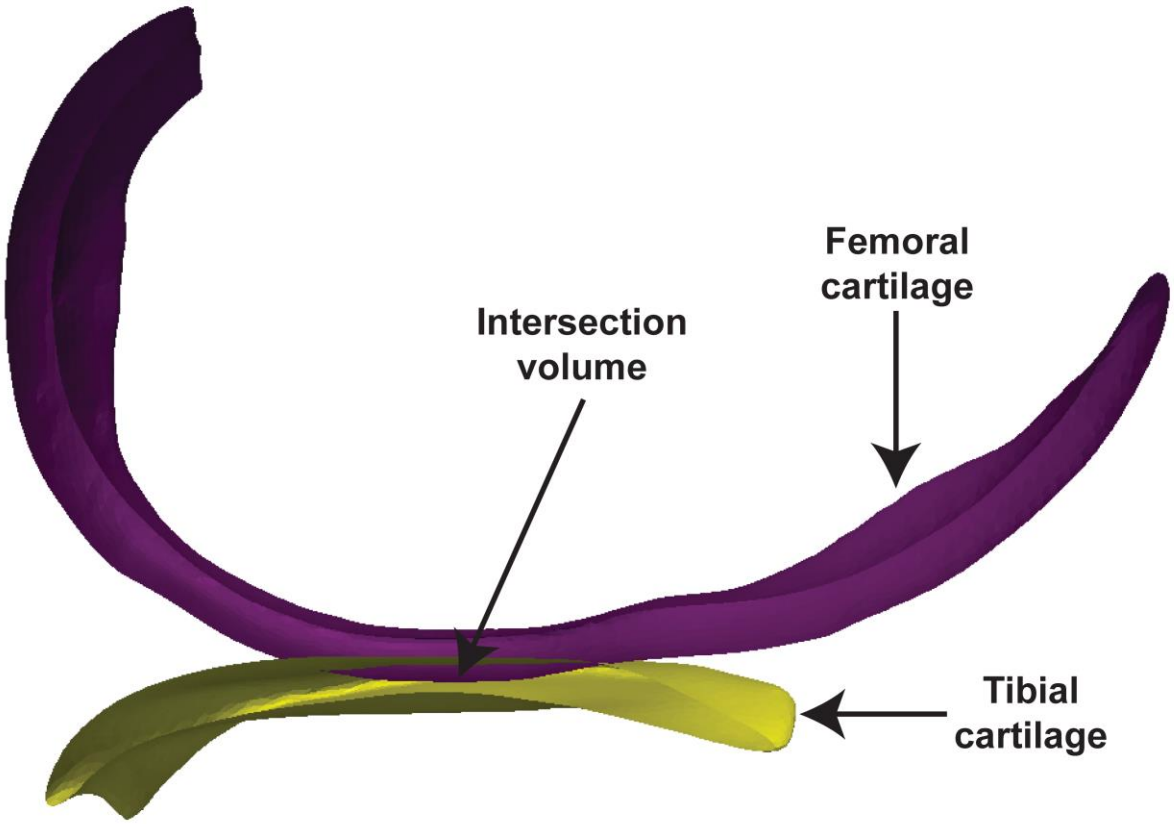


Figure 8: *In situ* contact area analysis (ISCAA) to determine the contact area, defined as the intersection between femoral and tibial cartilage, by co-registering the MRI-acquired cartilage models with DSX-acquired bone models.

For the FE models, the contact centroid ($C_{MRI}$ or $C_{DSX}$) was found by projecting the tibial cartilage on the aforementioned least-squares-fit plane and determining the geometric center in two dimensions (2D). For the ISCAA, the $C_{ISCAA}$ was found by discretizing the contact area into grid sections (size: 0.368 $mm^2$) and then identifying the section with the smallest weighted-average Euclidean distance to all other sections. Numerically, $C_{ISCAA}$ was located by the grid section ID ($i$) resulting from the following optimization procedure:

$$\underset{i}{\operatorname{argmin}} \sqrt{\sum_{j=1}^{N} \frac{s_{ij}^2}{d_i^2}} \tag{1}$$

where $s$ is the distance from one grid section $i$ to another grid section $j$; $d$ is the localized cartilage depression (i.e., the depth of overlap) at a grid section, and $N$ is the total number of grid sections. Note that when cartilage depression $d$ is uniform across the entire contact area, the solution from Eq. (1) would be the geometric center as in the case for $C_{MRI}$ and $C_{DSX}$.

A sensitivity analysis was performed to assess how sensitive $C_{MRI}$ and $C_{DSX}$ predictions would be to changes in assumed material properties of the articular cartilage, menisci and meniscal roots. Seven material property values (elastic modulus and Poisson's ratio of articular cartilage, elastic modulus and Poisson's ratio of meniscus in the circumferential direction, elastic modulus and Poisson's ratio of meniscus in the axial and radial directions, spring stiffness of the meniscal roots) were each varied by ±5% and ±10%, resulting in a total of 28 model variants.

## 2.3 RESULTS

When overlaying the FE model predictions for contact centroid with the ISCAA results, the DSX-based position models were in better agreement with the ISCAA results compared to MRI-based position models, as evidenced in Figure 9 by the alignment of the FE cartilage-to-cartilage contact area prediction with the areas of greater contact depth in the ISCAA.

With $C_{ISCAA}$ as the benchmark estimate for the contact centroid, $C_{DSX}$ predicted the contact centroid more accurately than $C_{MRI}$ (Figure 10). The mean absolute distance from $C_{FE}$ to $C_{ISCAA}$ was 6.395 mm (SD: 2.296 mm, range: 3.242 mm to 8.234 mm) for the MRI-based FE models, and 0.747 mm (SD: 0.457 mm, range: 0.205 mm to 1.307 mm) for the DSX-based FE models. $C_{DSX}$ estimate was closer to $C_{ISCAA}$ by 85% (±17%), on average, than $C_{MRI}$ (See Table 2).

Once the model in the DSX-based position was verified, cartilage-to-cartilage contact area between the femoral and tibial cartilage (reported as a percentage of the superior surface area of the tibial cartilage), maximum compressive stress and maximum contact pressure were extracted from the FE results and compared between the meniscectomized and healthy knees (Table 3). All three variables, in both the lateral and medial compartments, were greater for the meniscectomized knee compared to the healthy knee. It was also noted that the differences in these three variables between healthy and meniscectomized states were much greater in the lateral compartment than in the medial compartment.

The sensitivity analysis showed that variations of material properties by ±5% and ±10% had no marked effect on the average model-predicted contact centroid locations (Figure 11). The conclusion that the DSX-based model outperformed the MRI-based model and provided accurate predictions holds for the range of material property variations considered.

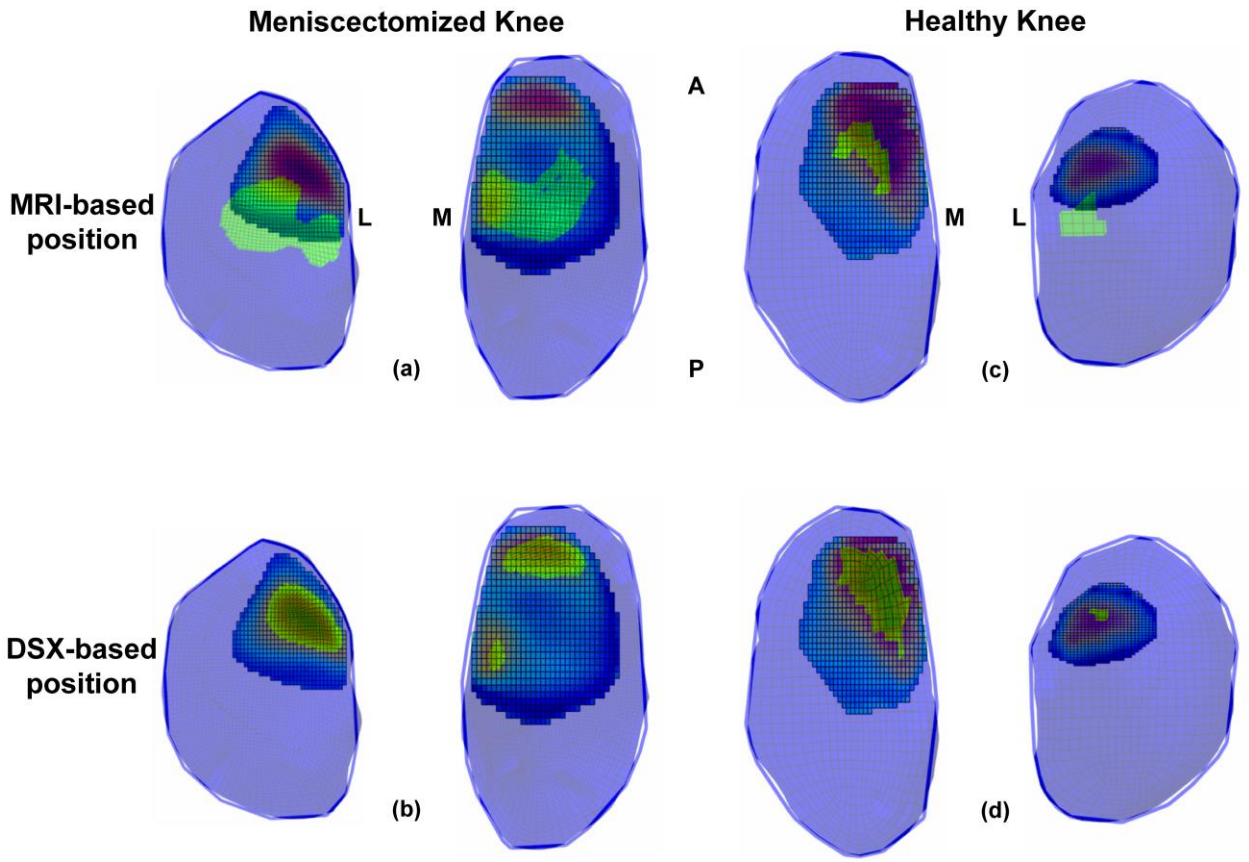


Figure 9: Left: meniscectomized knee ISCAA results overlapped with (a) MRI-based position and (b) DSX-based position FE model predictions. Right: healthy knee ISCAA results overlapped with (c) MRI-based position and (d) DSX-based position FE model predictions. The green area represents the FE model cartilage-to-cartilage contact area predictions, while the other colors are the color-coded ISCAA estimate. Penetration depth increases from blue to red. M = Medial, L = Lateral, A = Anterior, P = Posterior.

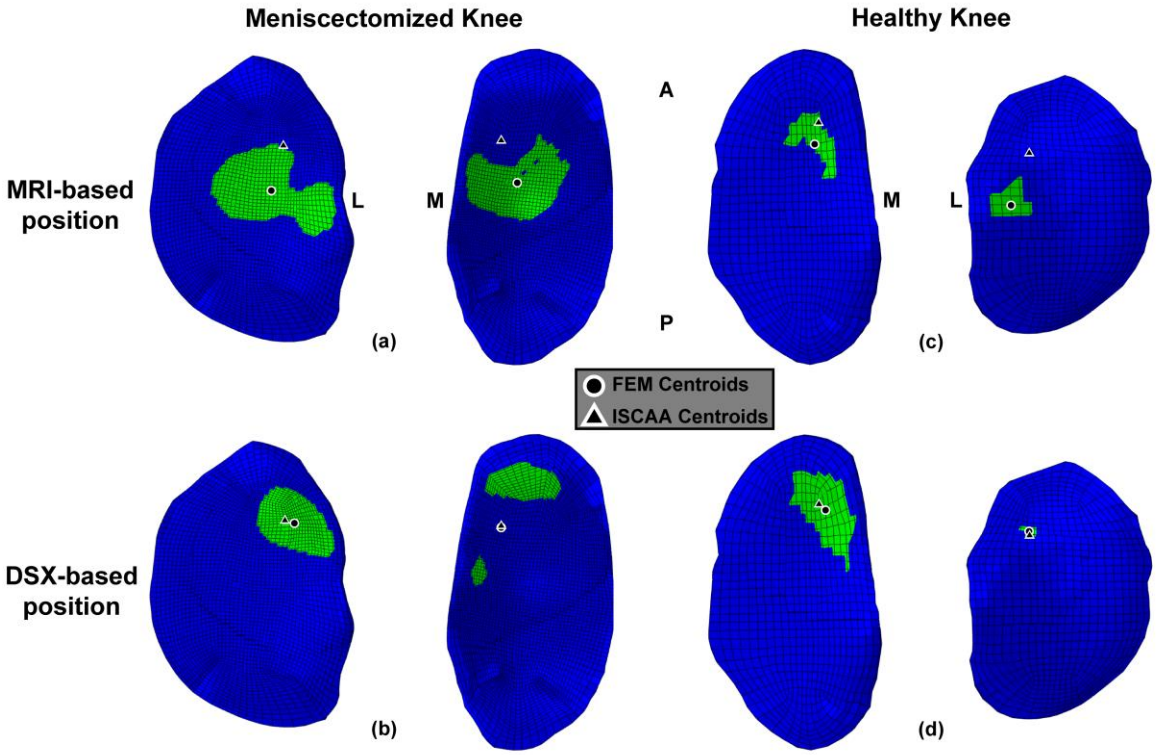


Figure 10: Left: contact centroid of ISCAA estimation and (a) MRI-based and (b) DSX-based FE model predictions for meniscectomized knee plotted on FE tibial cartilage. Right: contact centroid of ISCAA estimation and (c) MRI-based position and (d) DSX-based position FE model predictions for healthy knee plotted on FE tibial cartilage. M = Medial, L = Lateral, A = Anterior, P = Posterior.

Table 2: Distances (mm) between FE-predicted and ISCAA-estimated contact centroids

| | *Meniscectomized Knee* | | *Intact Knee* | |
|---|---|---|---|---|
| | Lateral Compartment | Medial Compartment | Lateral Compartment | Medial Compartment |
| MRI-based FE model | 7.95 | 6.15 | 8.23 | 3.24 |
| DSX-based FE model | 0.84 | 0.21 | 0.64 | 1.31 |

Table 3: DSX-based FE model predictions of cartilage-to-cartilage contact area, maximum contact and compressive stresses in meniscectomized and healthy knees

| | | *Meniscectomized Knee* | *Healthy Knee* |
|---|---|---|---|
| Cartilage-to-Cartilage Contact Area (%) | Medial | 8.3 | 8.2 |
| | Lateral | 5.8 | 0.4 |
| Maximum Contact Pressure (MPa) | Medial | 2.95 | 2.69 |
| | Lateral | 4.32 | 0.70 |
| Maximum Compressive Stress (MPa) | Medial | 2.86 | 2.27 |
| | Lateral | 3.96 | 0.56 |

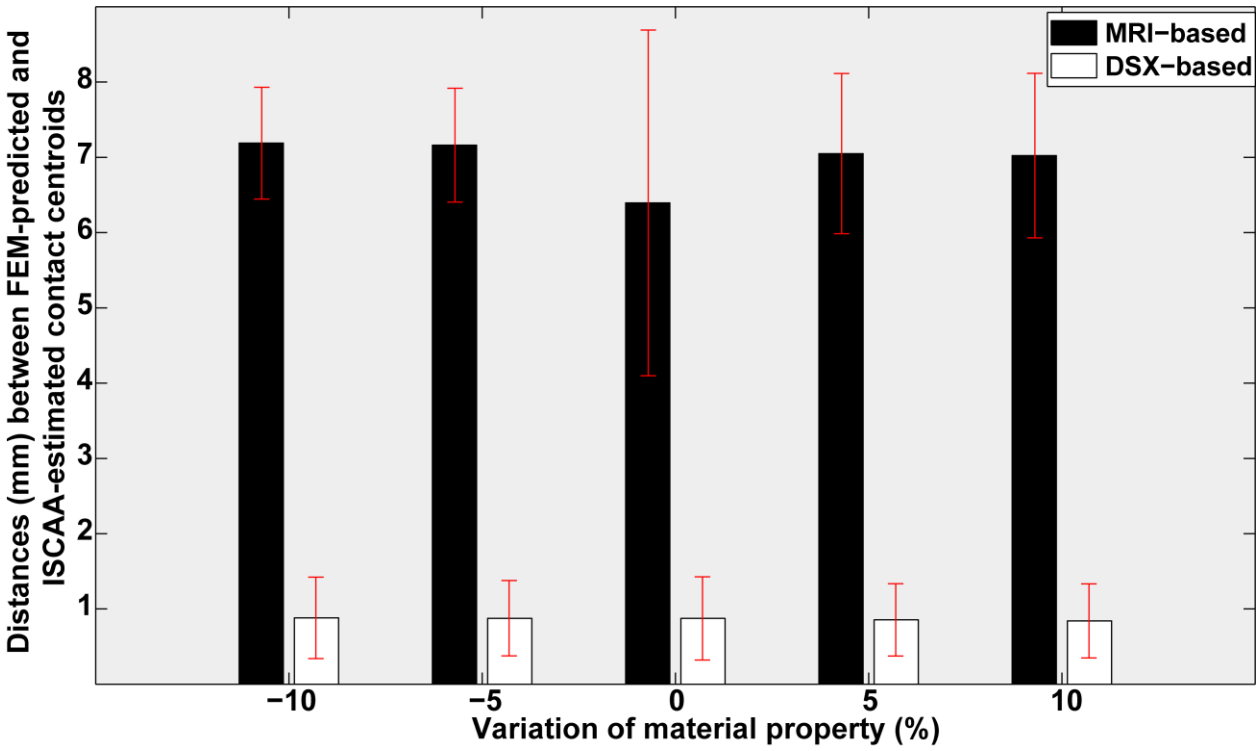


Figure 11: Average distances between FE-predicted and ISCAA-estimated contact centroids at different levels of material property variation for both MRI-based and DSX-based models.

## 2.4 DISCUSSION

The current study presents a novel approach to creating patient-specific FE models of the TF joint. This approach distinguishes itself from past efforts in two ways: (a) physiologically realistic weight-bearing states are modeled with high morphological and kinematic fidelity, and (b) the model is verified, *in vivo*, with a unique technique using the patient's own data.

The FE model of the patient in a standing posture, developed by integrating CT, MR and DSX images, was compared to an MRI-based FE model incorporating supine kinematics – a technique applied in past FE studies investigating TF mechanics [32, 33]. The contact centroid was used as a benchmark variable to discern the differences between the two FE models. The contact centroid was selected as a variable for verification/comparison since contact pressure and stress are currently infeasible to measure *in vivo* without surgically invasive procedures (which would also inevitably alter the characteristics of the contact itself). Further, accurate material properties, which are difficult to determine *in vivo* for the various components in the TF joint, are necessary for prediction of contact pressure and stress. In contrast, the contact centroid remains largely unaffected by the choice of material properties.

Application of highly accurate task-specific kinematics is critical for achieving accurate FE model predictions, as demonstrated by results from the current study. Creating a model in a weight-bearing state using non-weight-bearing kinematics [32, 33] incurs an artifact of joint congruity change, as evidenced by the differences in predicted contact area as well as the contact centroid. This could compromise the accuracy of predictions of the TF mechanical response and potentially obscure the true effects of structural alteration due to an injury or treatment. Customized loading devices have been used to emulate weight-bearing conditions during the

MRI scan [43, 77] but these alternatives are much less flexible in accommodating a variety of functional kinematics as compared to the dynamic X-ray imaging we used.

Experimental studies by Bingham et al. [78], Li et al. [79], and Van de Velde et al. [80] using biplane X-ray images of subjects in a full-extension weight-bearing position have showed that the contact centroids lie anterior to the anterior-posterior (AP) midline of the cartilage for both the lateral and medial compartments. Contact centroid estimation by the DSX-based model in the current study was consistent with those previous findings. However, studies using a supine position from MR imaging have provided different and often inconsistent estimates. For example, Perie et al. estimated the contact location to be anterior in the medial compartment, but toward the center in the lateral compartment, based on estimates of hydrostatic stress distribution from a supine MRI-based FE model of a healthy knee [33]. The discrepancy in the location of contact in the lateral compartment is similar to the prediction from the MRI-based FE model of the healthy knee in the current study. In contrast, experimental investigations by Shefelbine et al. [77] and Von Eisenhart-Rothe et al. [81] predicted the contact centroid to be posterior in the medial compartment and anterior on the lateral side with respect to the AP midline of the cartilage. A collective look at these studies conclusively establishes the potential for erroneous predictions when FE models rely on non-task-specific kinematics. Small changes in the positioning of the bones can cause substantial inaccuracies in FE model predictions, as shown by a previous sensitivity analysis [43].

The demonstration of a viable approach to verifying FE model predictions using subject-specific data is another unique contribution of this study. To our knowledge, there has not been any TF joint FE model employing a subject's own *in vivo* data to verify the model predictions. Peña et al. [53-55] developed several 3D FE models that considered *in vivo* functional

kinematics using weight-bearing MRI, but all of these models lacked validation or verification against data from the same subjects. Instead, verification was done by comparing the model results with literature data, some of which were based on *in vitro* cadaveric data. Considering the morphometric variations across individuals [40] and the discrepancies between *in vitro* and *in vivo* modalities in relation to sometimes subtle effects or differences, conventional verification can serve at best as a qualitative "reality check." With access to or the ability to acquire *in vivo* data, validating a subject-specific FE model by the subject's own data obviates errors arising from inter-individual morphological variations. As *in vivo* measurements of joint pressure and stress continue to be a formidable challenge, we believe the *in situ* contact area analysis proposed in the current study offers a viable alternative for quantitative verification of subject-specific FE models based on *in vivo* data.

Once the validity has been established, the model can be used with confidence to analyze the contact pressure and stress distribution in the joint complex. The subject modeled in this work had previously undergone a meniscectomy of the lateral meniscus on the left knee. The predicted cartilage-to-cartilage contact area, maximum contact pressure and maximum compressive stress in both the lateral and medial compartments were all greater in the meniscectomized knee than in the right, healthy knee during the static, standing trial. The difference was most evident in contact area in the lateral compartment. The trends found in this study—increased cartilage-to-cartilage contact area, increased maximum contract pressure and increased maximum compressive stress in the meniscectomized versus healthy knee—were consistent with prior reports based on FE analysis [46, 55-57].

While the contact centroid locations predicted by the FE model in DSX-based bone positions were in close agreement with those from the ISCAA, the actual contact area resulting

from the ISCAA was noticeably greater than the area predicted by the corresponding DSX-based FE model. This discrepancy may be attributable to two simplifying assumptions. First, in the ISCAA, the intersection between non-deformed cartilage volumes was assumed to represent the total volume in contact (i.e., experiencing stress). Had the deformation been taken into account, which is not yet achievable *in vivo*, the total volume or area in contact would likely be smaller, considering there would be deformed but non-contacting cartilage areas. Second, material properties used in the FE models were taken from literature on the subject of TF FE modeling, which may have contributed to the inaccuracy in prediction of contact area. *In vivo* subject-specific material properties remains the "holy grail" in biomechanics and having such property values for model development as well as validation would greatly reduce the putative error caused by use of generic "one-size-fits-all" data. It must be pointed out, nevertheless, that for a "within-model" comparative evaluation as done in the current study, the use of generic but consistent property values would be much less consequential, as confirmed by the sensitivity analysis conducted.

The cruciate ligaments (ACL, PCL) and collateral ligaments (MCL, LCL) were not included in the models in this study. It is understood that the ligaments play a central role in maintaining joint stability and therefore can affect the kinematics [82]. Inclusion of these ligaments in the DSX-based models would not have any effect on the kinematics, which was prescribed from experimental data. Inclusion of the ligaments in the MRI-based models might have an effect on the contact centroid predictions as the model permitted a large number of DOFs. Given that the MRI-based models saw only small femoral movement relative to the tibia (displacement < 1 mm) in response to the quasi-static loading, and that the standing position is considered the most "neutral" position in terms of ligament tensions and effect, we believe the

effect would be minimal. However, caution must be exercised when the proposed methodology is applied to modeling a joint in more dynamic acts and/or deviate positions. Another limitation of this study was the assumption of the loading condition applied to the TF joint. One-half of the body weight was administered only in the axial direction. Although we elected to use a simple loading scenario in order to minimize possible interaction effects on predicted joint mechanical responses and loading "bias" in model comparison, the actual loading would be more complex than a uniformly applied axial load. Our ongoing work involves the use of a musculoskeletal dynamic modeling tool OpenSim [83] to determine a more realistic ensemble force input for the FE model.

## 2.5 SUMMARY

In this chapter, it was discussed how computed tomography, magnetic resonance imaging and dynamic stereo-radiography data were used to develop subject-specific FE models of the TF joint. Two approaches of integrating kinematics into the models were compared using a novel ISCAA technique that employed subject-specific data, and the use of the contact centroid on the tibial cartilage showed the importance of utilizing task-specific kinematics when building FE models. The material property sensitivity analysis indicated that the contact centroid, used to verify the models, is not highly sensitive to the choice of material properties, thus the properties chosen were acceptable. Preliminary results of the verified model, assumptions used for the ISCAA, limitations of the study and directions for future studies were then discussed.

In Chapter 3, we will apply the previously verified models to study the effects of meniscectomy on the TF intra-articular contact mechanics during a decline walking task. Subject- and task-specific kinematics will be developed through the use of kinematics from DSX and skin surface markers, and from ground reaction forces. These elements will be applied to a musculoskeletal dynamic model in order to acquire TF joint compressive forces. These forces, along with corresponding kinematics from DSX measurements, will be applied to the FE models using a sequential quasi-static sequence. The resulting intra-articular contact mechanics will be collected and a comparison between the partially meniscectomized and healthy contralateral knees will be made.

# 3.0 APPLICATION

## 3.1 INTRODUCTION

Disruption of the meniscus, such as partial or complete removal by a meniscectomy, has been shown to lead to degenerative changes of the TF articular cartilage and eventually OA [18, 84, 85]. How aberration of TF joint function due to injury or treatment (e.g., meniscectomy) relates to the "wear-and-tear" degenerative changes of articular cartilage in the knee continues to intrigue clinicians and researchers alike. Assessing the joint mechanical consequences of meniscectomy can provide a better understanding of the relationship between treatment of injury and the onset as well as progression of articular cartilage damage.

Two important and inter-related aspects of changes in TF joint function due to injury or treatment are joint kinematics/kinetics and intra-articular contact mechanics. Small changes in kinematics can potentially result in large alterations in contact stress and pressure distribution patterns, possibly instigating degenerative changes in the joint [43]. However, small changes in kinematics may not be detected accurately enough to afford valid prediction of possible mechanical markers of degenerative changes. Furthermore, it has been shown that limbs with a partial meniscectomy have greater levels of flexor-extensor co-contraction which might lead to an increased total muscle force in the knee joint [11]. Hence intra-articular contact mechanics

must be examined in conjunction with joint kinematics/kinetics in order to fully understand the effects of meniscectomy on TF mechanical joint function.

One potentially measurable aspect of TF intra-articular contact mechanics is the maintenance of joint congruency [45], as indicated by factors such as cartilage-to-cartilage contact area, contact pressure and compressive stress, which can be assessed using finite element (FE) modeling. Modeling techniques, such as FE modeling, have demonstrated effectiveness in evaluating joint congruency in the meniscectomized and healthy TF joint [46, 53-55, 58, 70, 72, 86-89].

Most *in vivo* TF FE studies of the effects on meniscectomy on the mechanical function of the joint were limited to a static, standing weight-bearing position [46, 54, 55, 58, 64, 70, 86]. These studies have shown that meniscectomized TF joints, when compared to healthy joints, have increased levels of compressive and shear stresses in both the articular cartilage and menisci. Although such information is valuable in understanding the effects of meniscectomy in a static standing position, it lacks important details regarding the effects throughout the range of motion of an activity of daily living, which would provide a more relevant context for exploring the benefits and disadvantages of meniscectomy for both researchers and clinicians [70, 86]. Recent *in vivo* studies have modeled meniscectomy and integrated non-subject-specific gait kinematics and kinetics [72, 87]. The precision of developed models for such analysis is contingent upon accurate definitions of the geometry and kinematics/kinetics experienced by the joint [29, 88], therefore making the inclusion of subject-specific kinematics and kinetics vital for precise model predictions. Injury and treatment of the menisci can cause structural changes in the joint, thereby modifying the kinematics and kinetics of the joint complex [6, 13]. Netravali et al. observed the differences in the six degrees of freedom of the TF joint between subjects with

a partial medial meniscectomy and healthy contralateral limb using an opto-electronic system and found significantly greater external rotation and significantly less interval range of motion in the meniscectomized limb compared to the contralateral limb [6]. Therefore, use of non-subject-specific kinematics can potentially obfuscate the changes in the joint due to the injury or treatment being simulated.

In this study, we aimed to investigate alterations in the TF intra-articular contact mechanics after a unilateral partial meniscectomy of the lateral meniscus using a previously verified subject-specific FE technique based on *in vivo* morphological, kinematic and kinetic measurements. Three-dimensional (3D) skeletal kinematics were acquired using dynamic stereo-radiography (DSX), while TF joint compressive forces were found using a subject-specific musculoskeletal dynamic model developed with OpenSim [83]. These kinematic and kinetic inputs were applied to the subject-specific FE model for a sequence of time points within the stance phase of a decline walking task, which was selected due to the greater shear forces experienced in the TF joint when compared to level gait [90]. We believe the results will show a greater cartilage-to-cartilage contact area in the meniscectomized compartment compared to the other three compartments at each time point, and greater maximum compressive stress and contact pressure in both compartments in the meniscectomized knee compared to the healthy knee at each time point.

## 3.2 METHODS

### 3.2.1 Data Acquisition

We used data of a 19 year old female subject (56.2 kg, 169.5 cm) who participated in an IRB-approved meniscus allograft transplantation study, who had previously undergone an arthroscopic partial meniscectomy of the lateral meniscus in the left leg. To acquire 3D TF skeletal kinematics data, a DSX system with a precision of 0.2 mm in translation and 0.2° in rotation was used [49]. Whole body kinematics was also captured at the same time using an 8-camera surface-based motion capture system (VICON, Oxford, UK) to be used to aid in determining task-specific kinetics. Kinematical data was captured while the subject preformed the desired task on an instrumented dual belt treadmill (Bertec Corp., Columbus, Ohio, USA), which has the ability to record 3D ground-reaction forces for each half of the treadmill independently. The downhill walking trial data used in this study were collected while the subject walked down an inclined treadmill of 15° at a speed of 1 m/s (Figure 12). The decline walking task was selected due to the increased TF shear force in the joint as compared to level walking [90] in order to elicit differences between the healthy and meniscectomized TF joints. A handrail was provided for the subject for safety, but she was asked not to alter her normal gait by leaning on the rail. A bilateral computed tomography (CT) scan (GE Medical Systems Lightspeed Pro 16, Waukesha, WI, USA) and a sagittal 3D dual echo steady state water excitation (DESS-WE) MRI scan (Siemens Trio 3.0 Tesla, Washington DC, USA) were acquired while the subject was in a non-weight-bearing, supine position.

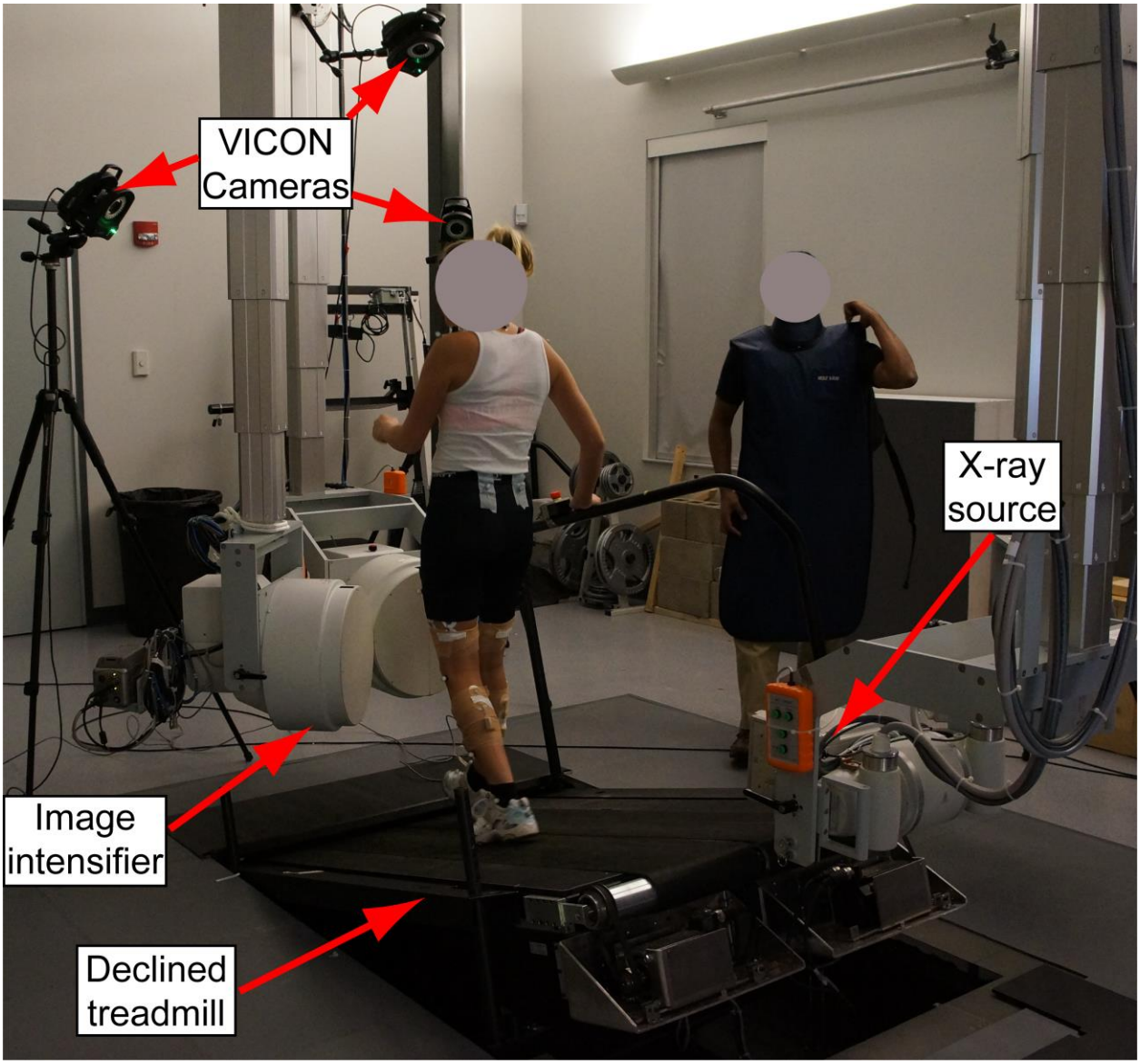


Figure 12: Subject, positioned within DSX system and VICON cameras, during decline walking task.

### 3.2.2 FE Model Construction

Three-dimensional models of the femur, tibia, femoral cartilage, tibial cartilage, and menisci were developed by importing the MRI data into Mimics 14.0. After generation of the 3D models, knee components were imported independently into TrueGrid for manual linear hexahedral meshing. Once meshed, each TF component was imported into Abaqus CAE 6.9, where they were combined into a single FE model for an implicit sequential quasi-static analysis.

### 3.2.3 Material Properties

Material properties of all tissues were taken from literature. In order to greatly reduce the computational time, the femur and tibia were modeled as rigid structures, which has been shown to have a minimal effect of the model predictions [22, 29, 32, 36, 46, 52-61, 67, 69, 70, 91]. With a time constant approaching 1500 seconds, articular cartilage is known to be an anisotropic, biphasic material [62, 63]. Due to the time independence of the compressive forces applied in his study, the biphasic response of the cartilage was ignored and a single-phase linear isotropic constitutive law was [62, 63]. Articular cartilage was therefore modeled as a homogeneous, elastic, linearly isotropic material [22, 29, 30, 32-34, 36, 43, 46, 47, 52-55, 57-61, 64-70, 91].

The circumferential fibers play a large role in the meniscal function; therefore, a homogeneous, elastic, linearly transversely isotropic constitutive law was used to model the menisci [1, 2, 10, 14, 29, 30, 32, 36, 37, 43, 47, 52, 56-58, 61, 65-67, 71, 72, 87]. Due to the quasi-static nature of the models, no time dependent effects for any of the model components were considered [32, 34, 35, 46, 52, 54, 57, 62-64, 70, 73, 74]. Linear springs were used to

model all four meniscal roots (lateral anterior, lateral posterior, medial anterior, medial posterior). Table 4 contains more details regarding the material properties chosen for the TF joint components.

### 3.2.4 Musculoskeletal Dynamic Simulation

In order to simulate downhill walking, task-specific kinetics were determined and incorporated into the FE model sequence. Using the downhill walking kinematics derived from the experimental testing, and the 3D ground reaction forces collected, OpenSim (SimTK, Stanford, California, USA) was used to determine joint reaction forces on the distal femur for both the meniscectomized and healthy knees during the downhill walking task.

A musculoskeletal dynamic model (Figure 13) that included 92 unique muscles and utilized 23-DOF [83, 92] was used in this study. The model was scaled based upon the anthropometric measurements and surface marker data from VICON. The knee joint was modeled as a 1-DOF joint, constraining three translations and both internal/external rotation and ab/adduction as cubic spline functions of knee flexion angle based on DSX measurement data. To derive full body joint angles, inverse kinematics was employed using both surface-based and DSX-measured kinematic data. Then a residual reduction algorithm was used to resolve any dynamic inconsistencies intrinsic in the model and experimental data. A computed muscle control algorithm was applied to compute the muscle excitations that constrained the model to track the specified joint kinematics [83], considering the task-specific ground reaction forces (GRFs) measured during testing, which allowed for predicted joint compressive forces to be

extracted [93, 94]. These forces can be seen in Figure 14 as a function of body weight (BW = 551 N) for both the meniscectomized and healthy knee.

Table 4: Material properties for each TF joint component for FE modeling (E = elastic modulus, $\nu$ = Poisson's ratio, $E_r$ and $\nu_r$ = elastic modulus and Poisson's ratio in radial direction, $E_z$ and $\nu_z$ = elastic modulus and Poisson's ratio in axial direction, $E_\theta$ and $\nu_\theta$ = elastic modulus and Poisson's ratio in circumferential direction and k = spring stiffness)

| *TF component* | *Material type* | *Value* | *Reference* |
|---|---|---|---|
| Bones (Femur/Tibia) | Rigid | N/A | [22, 29, 32, 36, 46, 52-61, 69, 91] |
| Articular cartilage (Femoral/Tibial) | Homogeneous<br>Elastic<br>Linear<br>Isotropic | E = 15 MPa<br>$\nu$ = 0.46 | [32, 36, 47, 52-55, 57, 58, 67, 70] |
| Menisci (Lateral/Medial) | Homogeneous<br>Elastic<br>Linear<br>Transversely Isotropic | $E_r$, $E_z$ = 20 MPa<br>$E_\theta$ = 140 MPa<br>$\nu_r$, $\nu_z$ = 0.2<br>$\nu_\theta$ = 0.3 | [52, 67, 72, 87] |
| Meniscal roots (Anterior/Posterior) | Homogeneous<br>Elastic<br>Linear | k = 2000 N/mm | [36, 46, 47, 52, 57, 58, 67, 72, 87] |

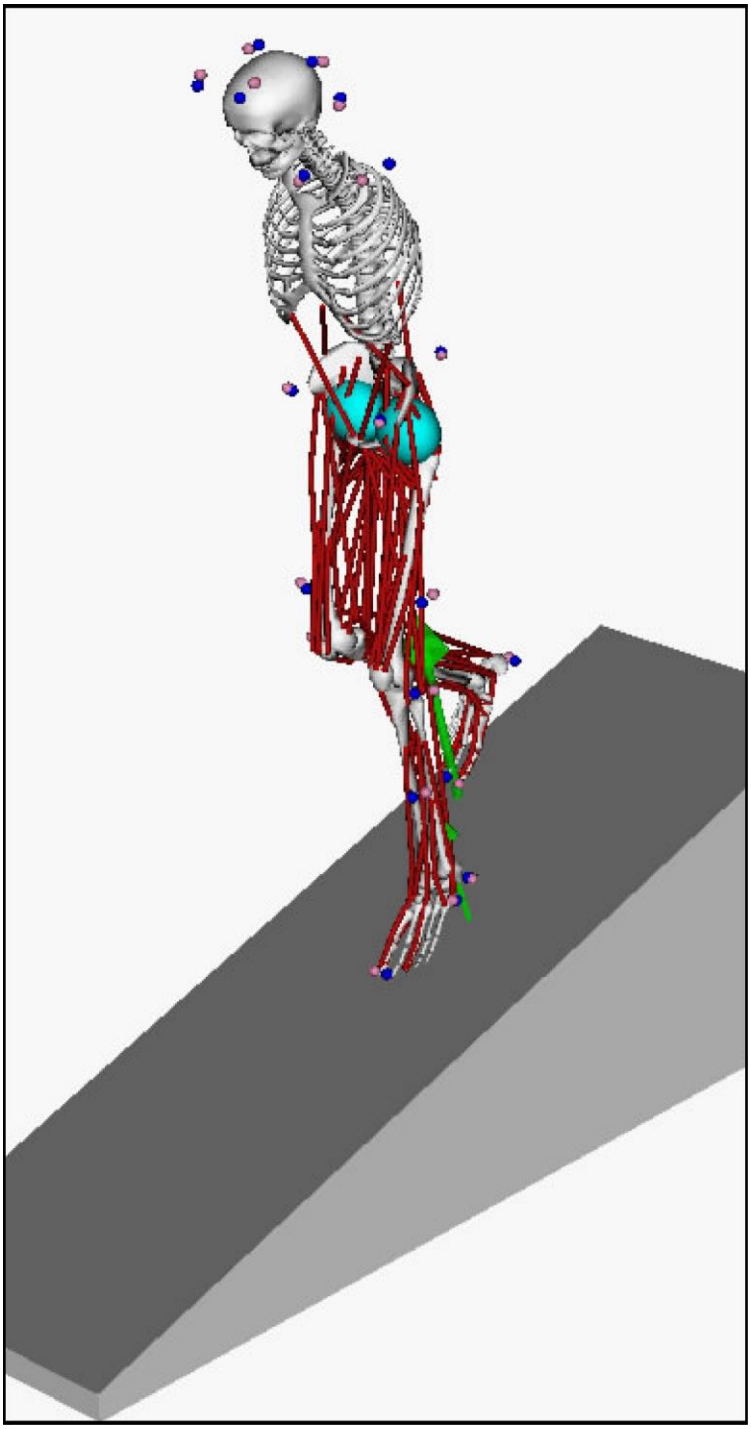

Figure 13: OpenSim simulation of a decline walking task using a 23-DOF musculoskeletal dynamic model.

### 3.2.5 Linking Musculoskeletal Dynamic Simulation and FE Model

The experimentally collected kinematics, along with the musculoskeletal dynamic simulation driven kinetics, were combined with the TF geometry to model a decline walking task. The FE models are in a supine, non-weight bearing position once the 3D geometry is developed from MRI. To incorporate the weight-bearing decline walking kinematics with the geometry, the coordinate system was adjusted, as described below.

For both the femur and tibia, the CT-based 3D model was co-registered to the MRI-based 3D model using Geomagic Studio 10. The average (± SD) error in the co-registration process for the bones was 0.472 (± 0.305) mm. This procedure output a transformation matrix from the CT coordinate system to the MRI coordinate system (CT-MRI). One output of the model-based tracking process was a transformation matrix from the laboratory coordinate system to the CT coordinate system (lab-CT) for each time point of the decline walking task. The lab-CT and CT-MRI transformation matrices for each respective bone at each desired time point were combined to yield a transformation matrix from the laboratory coordinate system to the MRI coordinate system (lab-MRI) at their respective time point. These transformations were then applied to each knee's MRI-based supine position FE model to create a model in the DSX-based weight-bearing decline walking position at each desired time point. The tibial side lab-MRI transformation was applied to the tibia, tibial cartilage and menisci, while the femoral side lab-MRI transformation was applied to the femur and femoral cartilage.

Heel-strike for both the kinematics and kinetics was found in order to align the two sets of data. Each knee was modeled at heel-strike and in increments of 0.05 seconds up to 0.30 seconds after heel-strike. In addition, the time points of the two peak compressive joint force values for each knee were selected for model development (Left leg: 2021 N at 0.06 sec after

heel-strike, 2241 N at 0.21 sec after heel-strike; Right leg: 2612 N at heel-strike, 2122 N at 0.20 sec after heel-strike). For the left, meniscectomized knee, a total of nine models were developed (heel-strike, 0 sec, 0.05 sec, 0.06 sec, 0.10 sec, 0.15 sec, 0.20 sec, 0.21 sec, 0.25 sec and 0.30 sec after heel-strike) and for the right, healthy knee, a total of seven models were developed (heel-strike, 0 sec, 0.05 sec, 0.10 sec, 0.15 sec, 0.20 sec, 0.25 sec and 0.30 sec after heel-strike). The corresponding kinematics and kinetics at each time point were combined with the FE model to create a quasi-static sequence modeling a subject- and task-specific downhill walking task.

For all the models, the tibia was fixed while the femur was allowed to translate axially in response to a compressive joint force applied to the proximal end of the femur. The only DOF allowed was an axial translation since the medial/lateral and anterior/posterior position of the femur relative to tibia is a final, known position from the experimental DSX-based 6-DOF data. This allowed the femur to settle into its final position in the axial direction in response to the force applied. Contact pairs, prescribed boundary conditions and the aforementioned force all contributed to the determination of the "final position" of each model. Both the femoral and tibial cartilage components were tied to their respective bone surfaces, while hard, frictionless contact was assumed for cartilage-cartilage and cartilage-meniscus boundaries [32, 52, 56, 57, 59, 61, 65, 67, 75]. A large-strain formulation was used for all models [60, 68, 69].

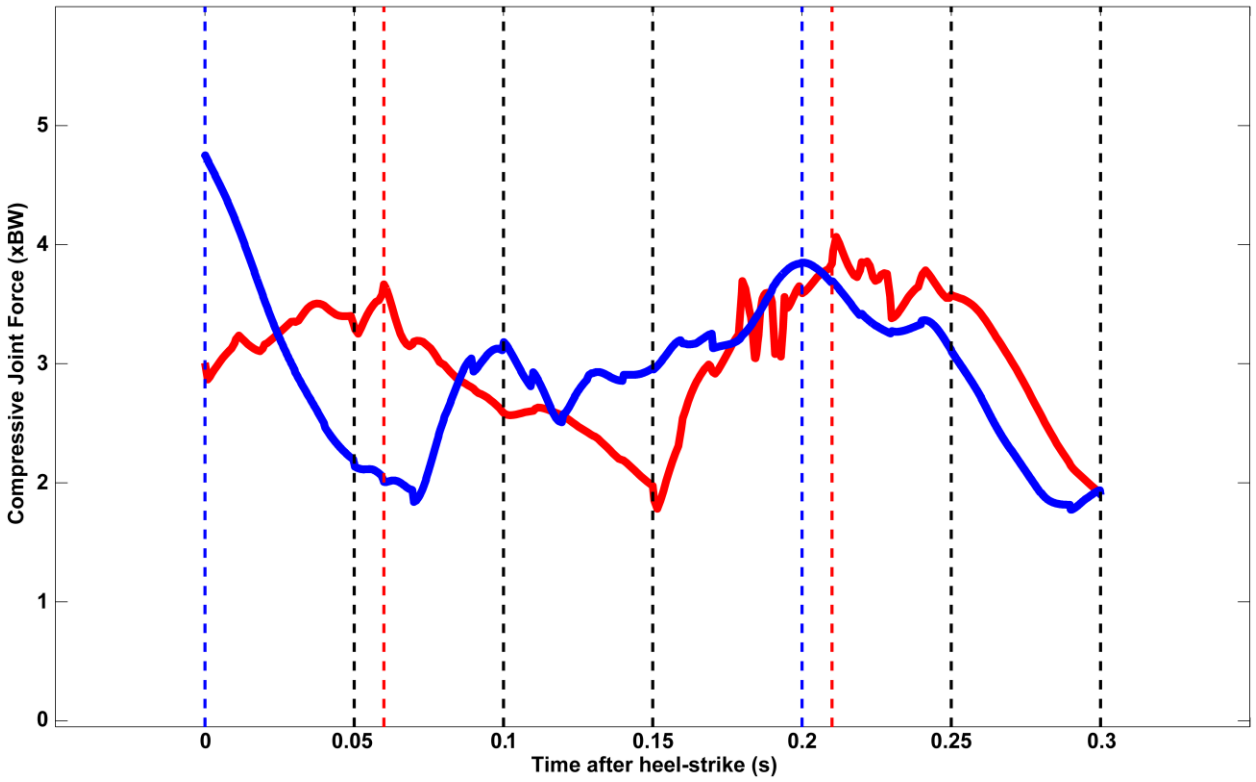


Figure 14: Solid red and blue lines are the time-varying OpenSim-predicted TF joint compressive forces for the meniscectomized and healthy knees, respectively. Red and blue dotted lines indicate peak joint compressive forces for their respective knees, while black dotted lines indicated additional modeled time points for both knees.

## 3.3 RESULTS

In order to measure joint congruency, the cartilage-to-cartilage contact area, maximum compressive stress, maximum contact pressure and maximum shear stress were observed in four different locations for each knee at each time point modeled: the right knee lateral compartment (RLC), the right knee medial compartment (RMC), the left knee medial compartment (LMC) and the left knee lateral compartment (LLC), which was the compartment with the partial meniscectomy. The cartilage-to-cartilage contact area in the LLC was greater than the contact area seen in the other three compartments, as expected after part of the meniscus is removed (Figure 15).

The maximum compressive stress on the tibial cartilage was greater in the LLC and in the RMC than in the other two compartments for the entire time (Figure 16a). The profiles for the maximum compressive stress in the LLC and RMC were very similar, with major differences in the very beginning of the stance phase, while the profiles for the other two compartments, the LMC and the RLC, also had similar profiles with the major differences occurring in the second half of the stance phase. In the second half of the stance phase, the maximum compressive stress in the LMC was much larger than that of the RLC, but still less than in the LLC and RMC. On the menisci, the profiles for maximum compressive stress in all four compartments were fairly similar, except in the LMC, which had a peak in the second half of the stance phase at the same time when the tibial cartilage experienced its peak (Figure 16b). There was also a large difference between the values at heel-strike, when the LMC and RLC experienced much greater values of maximum compressive stress than the other two compartments.

The maximum contact pressure on the tibial cartilage was greatest in the RMC or the LLC for the entire time. The RMC had a varying profile while the LLC showed a much more

consistent contour (Figure 17a). On the menisci, the compartments with the maximum predicted values of contact pressure were dissimilar than for the tibial cartilage (Figure 17b). Whereas the tibial cartilage saw the greatest values in the RMC or the LLC, the greatest values of maximum contact pressure on the menisci were mixed between the RLC, LMC and LLC, while the RMC had the smallest value of maximum contact pressure the majority of the time. The LMC showed the two greatest peaks of maximum contact pressure, one shortly after heel-strike and the other occurring in the second half of the stance phase.

The maximum shear stress seen by the tibial cartilage throughout the stance phase of gait was experienced in the RMC (Figure 18). The peak maximum shear stress in the RMC was seen in the first half of the stance phase, with a second smaller peak occurring in the second half of the stance phase. The other three compartments were varied, but each showed instances of peak maximum shear stress.

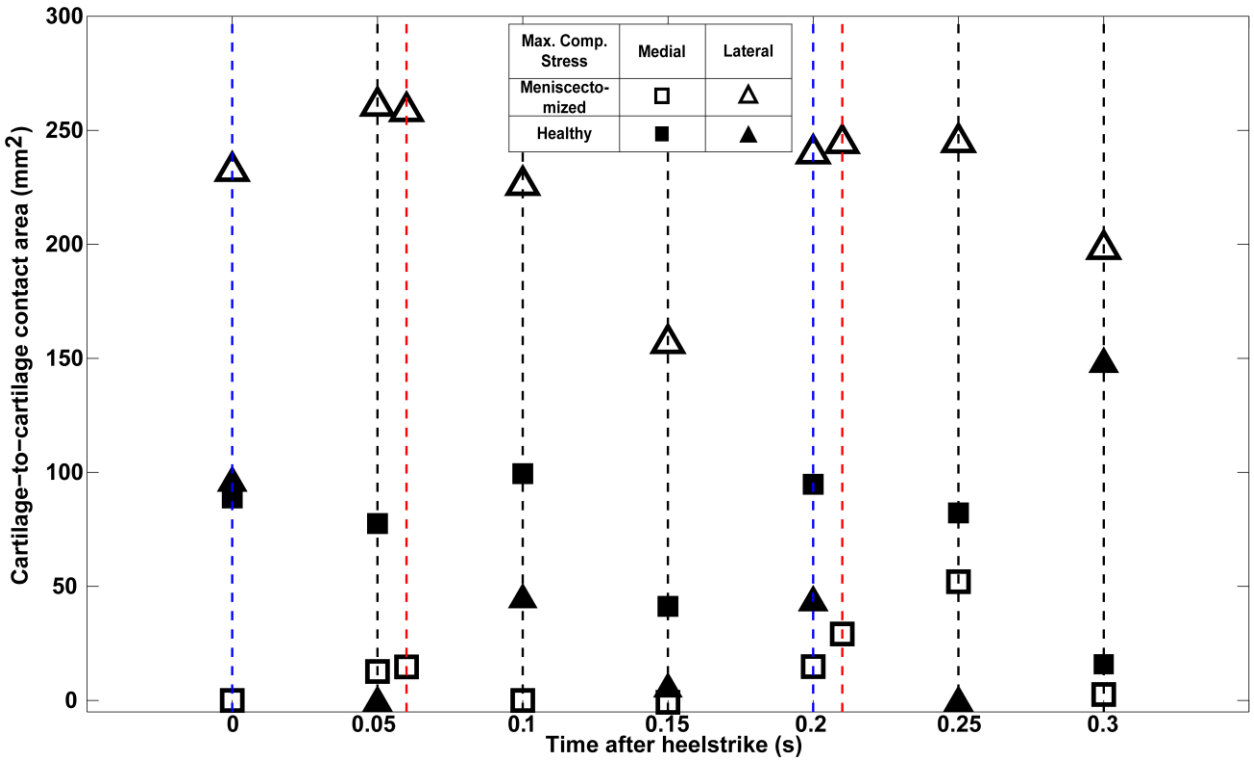


Figure 15: FE predicted cartilage-to-cartilage contact area.

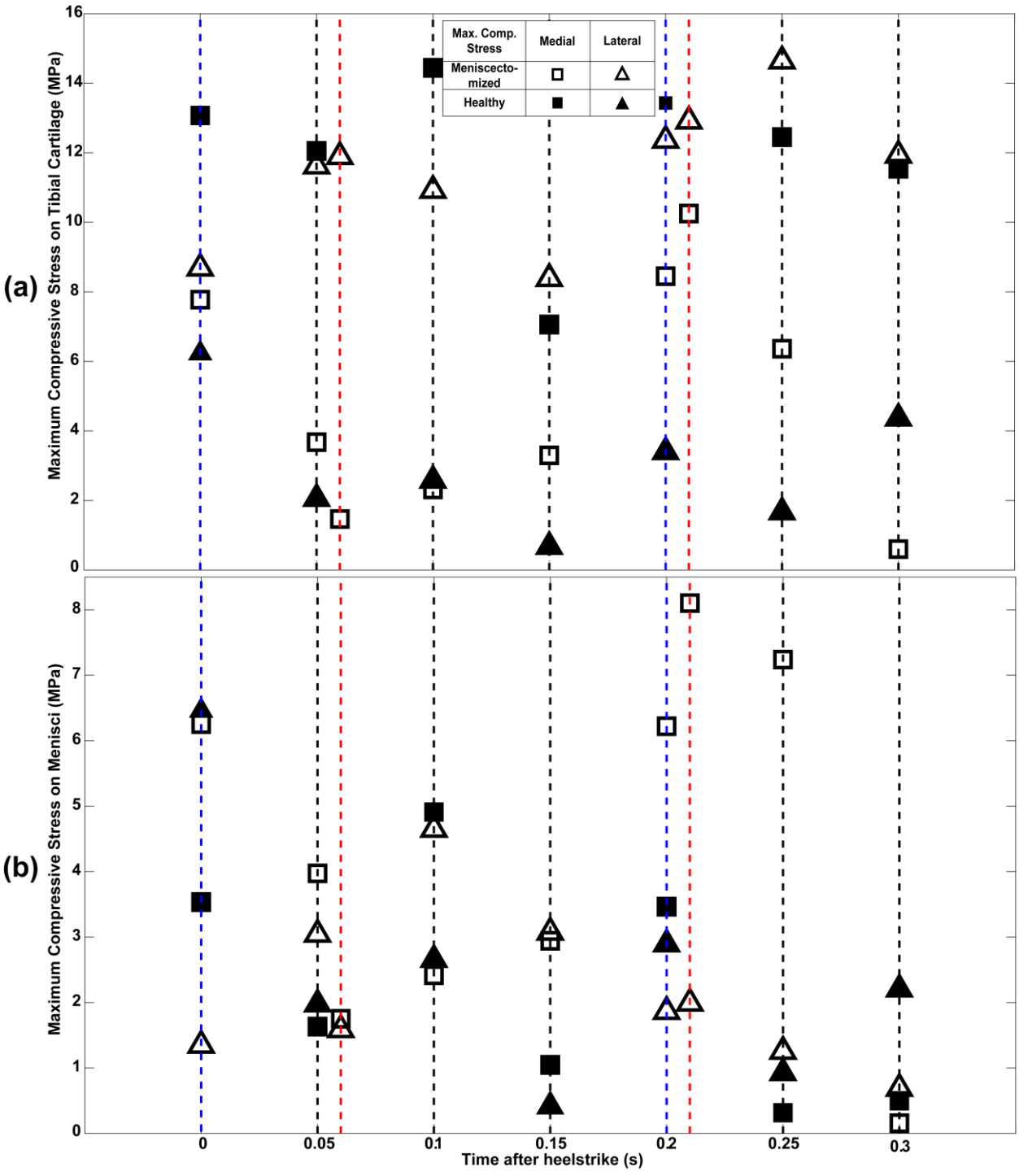


Figure 16: FE predicted maximum compressive stress on the (a) tibial cartilage and (b) menisci.

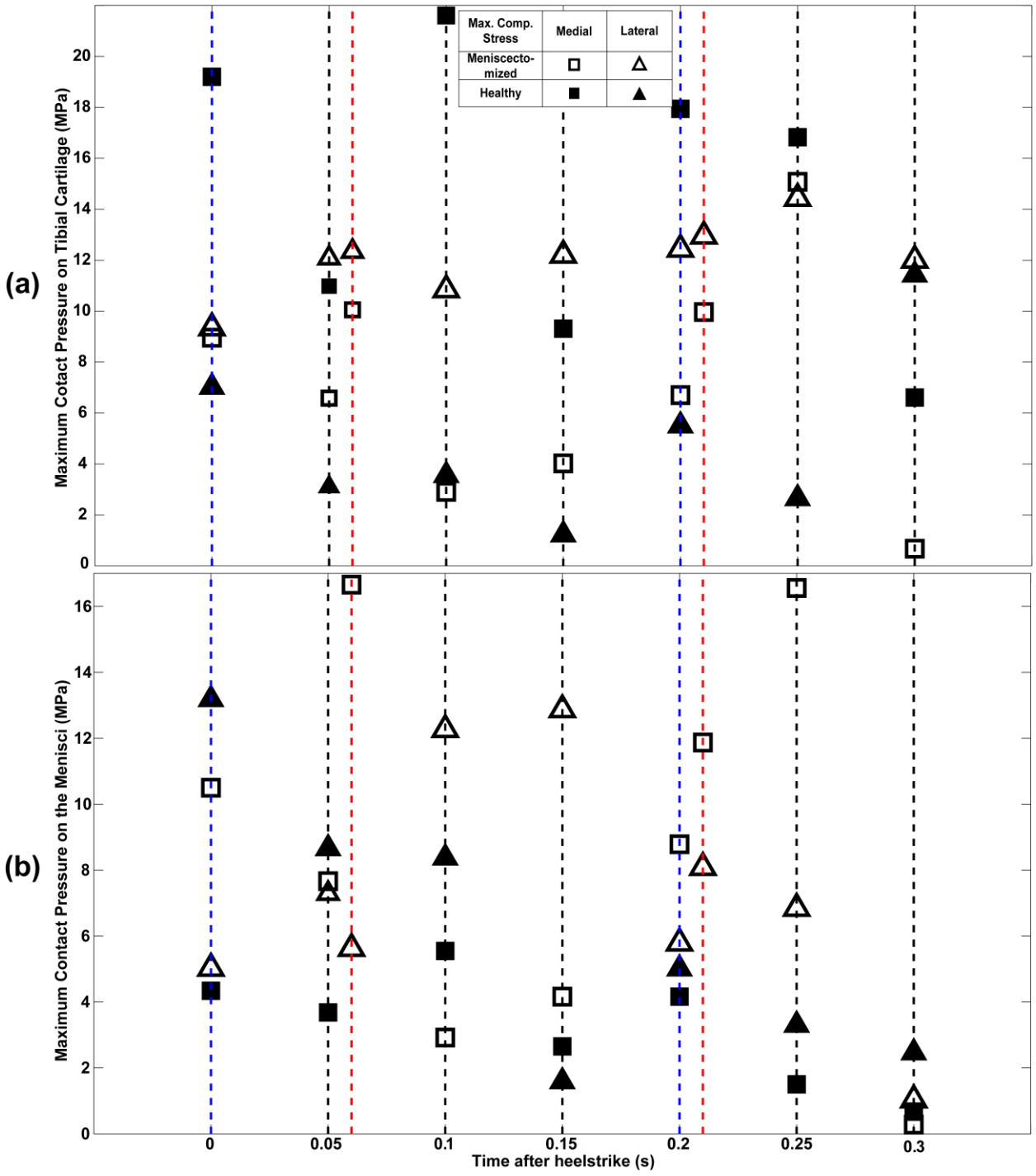


Figure 17: FE predicted maximum contact pressure on the (a) tibial cartilage and (b) menisci.

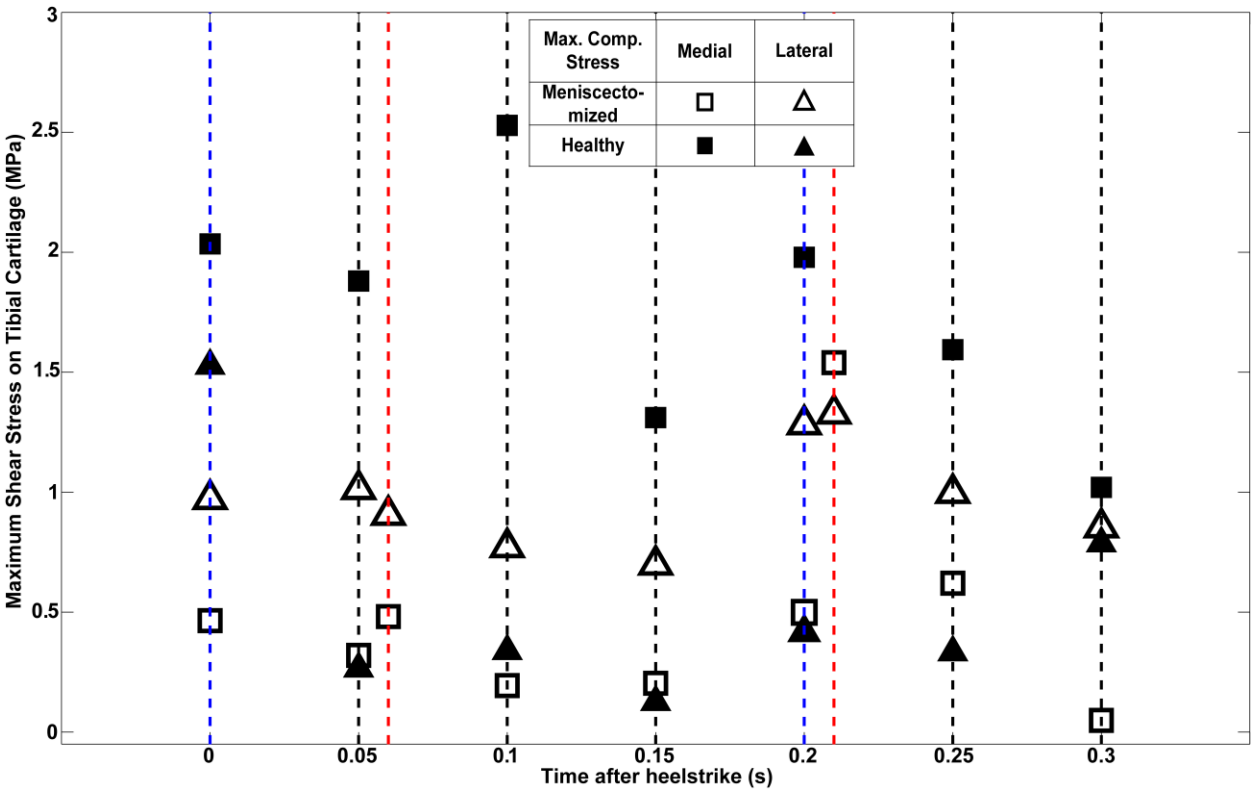


Figure 18: FE predicted maximum shear stress on the tibial cartilage.

## 3.4 DISCUSSION

The current study presents a method to create subject- and task-specific FE models of the TF joint and apply these models to the study of patho-mechanics, using partial meniscectomy as an example. This approach distinguishes itself from past studies in that it applies a sequential quasi-static method, rather than a static method, to FE model development while using subject-specific geometry and *in vivo* kinematics and kinetics, which are acquired from musculoskeletal dynamic modeling.

A previously verified FE model developed from MRI was integrated with high fidelity subject-specific kinematics from CT and DSX imaging, and combined with subject-specific kinetics developed using the OpenSim platform, to obtain subject- and task-specific models. This was done for both knees of a single patient who had previously undergone a left knee lateral partial meniscectomy, creating two sets of models, one for each leg. In order to simulate a decline walking task, multiple time points during the stance phase were chosen and static models were developed at these times with corresponding kinematics and kinetics, creating a sequential quasi-static modeling technique. Once the models were developed, the intra-articular contact mechanics were collected and compared between the meniscectomized knee and the healthy, contralateral knee throughout the stance phase of gait.

The greatest cartilage-to-cartilage contact area was seen in the meniscectomized compartment. This result is intuitive, as removing meniscus, which separates the tibial and femoral cartilage, would allow for more contact to occur. Although the cartilage-to-cartilage contact area increased after meniscectomy, we also saw that the total area of contact within the joint (cartilage-to-cartilage and meniscus-to-cartilage) decreased.

Our results have shown that the LLC (meniscectomized compartment) does not see the greatest maximum compressive stress throughout the entire stance phase. It was noted that either the LLC or the RMC had the greatest values for maximum compressive stress throughout the stance phase. Many previous studies simulating a static, standing weight-bearing position for the TF joint have seen an increase in the maximum compressive stress in the meniscectomized joint compared to the healthy joint [46, 54, 55, 58, 70, 86]. This result is not incorrect, but is not enough information for a clinician to make an informed decision whether or not to perform a meniscectomy. It lacks information regarding common everyday dynamics activities, such as walking. Information regarding intra-articular contact mechanics during a high-shear force inducing activity, which aids in the expedition of the onset of OA [95], can help better inform clinicians and researchers alike.

One previous study has seen an overall increase in the maximum compressive stress in the partially meniscectomized TF joint compared to the healthy TF joint throughout the stance phase of gait [72]. The FE model in that study lacked subject-specific kinematics and kinetics, and instead, generic healthy kinematics and kinetics were applied, which may have caused it to estimate inaccurate results. In the current study, it was noted that during the stance phase, the meniscectomized knee was in a valgus state while the healthy knee changes from valgus to varus. This finding may cause the maximum compressive stress patterns that we see in the models, and highlights the importance of subject- and task-specific FE modeling incorporating accurate skeletal kinematics and more realistic predictions of dynamic joint loading. Modeling results thus obtained through these simulations may offer better insights into the relationship between patho-mechanics and the development of OA in the knee.

The current study was limited to modeling of a single subject, which does not allow for any statistical analysis, and therefore limits the power of the findings. In order to truly produce an informed decision as to whether partial meniscectomy is an effective clinical tool in the treatment of meniscal injuries, and since FE modeling is a subject-specific technique, more subjects will need to be modeled in order to determine if there is one overall solution or if meniscectomy is truly a patient-by-patient decision. This study also used a quasi-static modeling sequence, which does not model every instance of time throughout gait, but rather choses certain time points, and ignores the effects of velocity and acceleration. This modeling technique may have caused an important time point to go unobserved, and therefore, may cause pertinent results to be unreported, while a lack of velocity and acceleration may affect the FE model predictions. A more effective method is to use a fully dynamic FE modeling technique, which captures every time point from start to finish, and which we plan on using in future studies.

## 3.5 SUMMARY

In this chapter, previously verified FE models of a partial meniscectomized and healthy knee of a single subject were applied to study the effects of meniscectomy on the intra-articular contact mechanics. Subject- and task-specific kinetics was developed for application to the FE models using a musculoskeletal dynamic model during a decline walking task. Once joint compressive forces were obtained, they were applied to the FE models, along with corresponding decline walking kinematics acquired from dynamic stereo-radiography using a sequential quasi-static model sequence. The time points for FE model creations were chosen to be at heel-strike and in

increments of 0.05 seconds up to 0.30 seconds, and two instances of maximum joint compressive force for each corresponding knee. Cartilage-to-cartilage contact area, maximum compressive stress, maximum contact pressure and maximum shear stress were compared between the lateral and medial compartments in the partial meniscectomized knee and the contralateral healthy knee. The results indicated that a partial meniscectomy has detrimental effects on not only the knee containing the partial meniscectomy, but also the contralateral healthy knee.

# 4.0 CLOSING

In summary, a FE model of the TF joint was developed from CT, MRI and DSX data *in vivo*, verified using subject-specific data and applied to study the effects that meniscectomy has on the mechanical function of the joint. The latter task was accomplished by incorporating a decline walking task with the previously verified models using sequential quasi-static modeling that incorporated subject- and task-specific kinetic inputs found using a musculoskeletal dynamic model.

This work provides new and useful information and techniques to the field of biomechanical research. A new method of FE model verification has been detailed in which the developed subject-specific model is compared to data from the same subject. This technique can be used to develop highly accurate subject- and task-specific models, and with proof of the accuracy of these models, will lead to more accurate and useful predictions.

The work also places an emphasis on the inclusion of subject- and task-specific inputs into the development of FE models to obtain results that are applicable in a research and clinical environment. Previous models have lacked specification of FE model inputs or have used non-subject-specific data, and the predictions from these studies are more likely to be error prone. Verification or validation of these studies was also taken from literature or *in vitro* studies, and while this can provide a basic reality-check into the model predictions, it cannot deliver a true verification or validation of the models.

The application of the verified models to a pathological example (meniscectomy in this case) will allow for better insight into the effects on the joint in question. Since different tasks require different movements of the body and different muscle inputs and since all people are physically unique, subject- and task-specific kinematics and kinetics allows for a more in-depth understanding for a particular subject. This specificity will allow for a treatment tailored to the patient, which hopefully will deliver a better clinical outcome. The use of a sequential quasi-static sequence using a subject- and task-specific approach provides better insight into the effects that meniscectomy has during a dynamic, everyday task. This knowledge will help clinicians decide if meniscectomy is an improvement over meniscal pathologies, such as tears.

The techniques detailed above, including the methods for FE development, verification and application are believed to be applicable to any articulating joint. The TF joint and meniscectomy are just one example of the power of FE modeling and its many applications. Further studies observing the TF joint are warranted due to the limited results found, which call for more improvements in the modeling process. Quasi-static modeling was used for the study of meniscectomy on mechanical joint function, but the data collected for both subject- and task-specific kinematics and kinetics is dynamic, and therefore, to get an even more accurate picture of the effects of meniscectomy, a dynamic FE modeling technique should be employed.

Another improvement in future studies will be a more realistic material structure applied to the soft tissues involved in the joint. In these studies, soft tissues, such as articular cartilage, were taken to be homogeneous, elastic and linear materials with no time-dependent effects. Although these simplified material properties are acceptable for the studies, they do limit the predictions made by the FE process. More advanced material properties, such as viscoelasticity,

can be applied to obtain a better understanding of how these soft tissues and their pathologies affect the mechanical joint function.

## BIBLIOGRAPHY


[1] Fithian, D. C., Kelly, M. A., and Mow, V. C., 1990, "Material Properties and Structure-Function Relationships in the Menisci," Clin Orthop Relat Res, 252), pp. 19-31.

[2] Vedi, V., Williams, A., Tennant, S. J., Spouse, E., Hunt, D. M., and Gedroyc, W. M., 1999, "Meniscal Movement. An in-Vivo Study Using Dynamic Mri," J Bone Joint Surg Br, 81(1), pp. 37-41.

[3] Greis, P. E., Bardana, D. D., Holmstrom, M. C., and Burks, R. T., 2002, "Meniscal Injury: I. Basic Science and Evaluation," J Am Acad Orthop Surg, 10(3), pp. 168-76.

[4] Poole, A. R., Kojima, T., Yasuda, T., Mwale, F., Kobayashi, M., and Laverty, S., 2001, "Composition and Structure of Articular Cartilage: A Template for Tissue Repair," Clin Orthop Relat Res, 391 Suppl), pp. S26-33.

[5] Buckwalter, J. A., Saltzman, C., and Brown, T., 2004, "The Impact of Osteoarthritis: Implications for Research," Clin Orthop Relat Res, 427 Suppl), pp. S6-15.

[6] Netravali, N. A., Giori, N. J., and Andriacchi, T. P., 2010, "Partial Medial Meniscectomy and Rotational Differences at the Knee During Walking," J Biomech, 43(15), pp. 2948-53.

[7] Jones, J. C., Burks, R., Owens, B. D., Sturdivant, R. X., Svoboda, S. J., and Cameron, K. L., 2012, "Incidence and Risk Factors Associated with Meniscal Injuries among Active-Duty Us Military Service Members," J Athl Train, 47(1), pp. 67-73.

[8] Paxton, E. S., Stock, M. V., and Brophy, R. H., 2011, "Meniscal Repair Versus Partial Meniscectomy: A Systematic Review Comparing Reoperation Rates and Clinical Outcomes," Arthroscopy, 27(9), pp. 1275-88.

[9] Lyman, S., Hidaka, C., Valdez, A. S., Hetsroni, I., Pan, T. J., Do, H., Dunn, W. R., and Marx, R. G., 2013, "Risk Factors for Meniscectomy after Meniscal Repair," Am J Sports Med, 41(12), pp. 2772-8.

[10] Aufderheide, A. C., and Athanasiou, K. A., 2004, "Mechanical Stimulation toward Tissue Engineering of the Knee Meniscus," Ann Biomed Eng, 32(8), pp. 1161-74.

[11] Dempsey, A. R., Wang, Y., Thorlund, J. B., Mills, P. M., Wrigley, T. V., Bennell, K. L., Metcalf, B. R., Hanna, F., Cicuttini, F. M., and Lloyd, D. G., 2013, "The Relationship between Patellofemoral and Tibiofemoral Morphology and Gait Biomechanics Following Arthroscopic Partial Medial Meniscectomy," Knee Surg Sports Traumatol Arthrosc, 21(5), pp. 1097-103.

[12] Durselen, L., Vogele, S., Seitz, A. M., Ignatius, A., Friederich, N. F., Bauer, G., and Majewski, M., 2011, "Anterior Knee Laxity Increases Gapping of Posterior Horn Medial Meniscal Tears," Am J Sports Med, 39(8), pp. 1749-55.

[13] Magyar, O. M., Illyes, A., Knoll, Z., and Kiss, R. M., 2008, "Effect of Medial Meniscectomy on Gait Parameters," Knee Surg Sports Traumatol Arthrosc, 16(4), pp. 427-33.

[14] Messner, K., and Gao, J., 1998, "The Menisci of the Knee Joint. Anatomical and Functional Characteristics, and a Rationale for Clinical Treatment," J Anat, 193 ( Pt 2)(pp. 161-78.

[15] Muriuki, M. G., Tuason, D. A., Tucker, B. G., and Harner, C. D., 2011, "Changes in Tibiofemoral Contact Mechanics Following Radial Split and Vertical Tears of the Medial Meniscus an in Vitro Investigation of the Efficacy of Arthroscopic Repair," J Bone Joint Surg Am, 93(12), pp. 1089-95.

[16] Rangger, C., Klestil, T., Gloetzer, W., Kemmler, G., and Benedetto, K. P., 1995, "Osteoarthritis after Arthroscopic Partial Meniscectomy," Am J Sports Med, 23(2), pp. 240-4.

[17] Rath, E., and Richmond, J. C., 2000, "The Menisci: Basic Science and Advances in Treatment," Br J Sports Med, 34(4), pp. 252-7.

[18] Seitz, A. M., Lubomierski, A., Friemert, B., Ignatius, A., and Durselen, L., 2012, "Effect of Partial Meniscectomy at the Medial Posterior Horn on Tibiofemoral Contact Mechanics and Meniscal Hoop Strains in Human Knees," J Orthop Res, 30(6), pp. 934-42.

[19] Voloshin, A. S., and Wosk, J., 1983, "Shock Absorption of Meniscectomized and Painful Knees: A Comparative in Vivo Study," J Biomed Eng, 5(2), pp. 157-61.

[20] Baratz, M. E., Fu, F. H., and Mengato, R., 1986, "Meniscal Tears: The Effect of Meniscectomy and of Repair on Intraarticular Contact Areas and Stress in the Human Knee. A Preliminary Report," Am J Sports Med, 14(4), pp. 270-5.

[21] Fukubayashi, T., and Kurosawa, H., 1980, "The Contact Area and Pressure Distribution Pattern of the Knee. A Study of Normal and Osteoarthrotic Knee Joints," Acta Orthop Scand, 51(6), pp. 871-9.

[22] Andriacchi, T. P., Briant, P. L., Bevill, S. L., and Koo, S., 2006, "Rotational Changes at the Knee after Acl Injury Cause Cartilage Thinning," Clin Orthop Relat Res, 442(pp. 39-44.

[23] Abraham, C. L., Maas, S. A., Weiss, J. A., Ellis, B. J., Peters, C. L., and Anderson, A. E., 2013, "A New Discrete Element Analysis Method for Predicting Hip Joint Contact Stresses," J Biomech, 46(6), pp. 1121-7.

[24] Guilak, F., and Mow, V. C., 2000, "The Mechanical Environment of the Chondrocyte: A Biphasic Finite Element Model of Cell-Matrix Interactions in Articular Cartilage," J Biomech, 33(12), pp. 1663-73.

[25] Adouni, M., Shirazi-Adl, A., and Shirazi, R., 2012, "Computational Biodynamics of Human Knee Joint in Gait: From Muscle Forces to Cartilage Stresses," J Biomech, 45(12), pp. 2149-56.

[26] Van Jonbergen, H. P., Innocenti, B., Gervasi, G. L., Labey, L., and Verdonschot, N., 2012, "Differences in the Stress Distribution in the Distal Femur between Patellofemoral Joint Replacement and Total Knee Replacement: A Finite Element Study," J Orthop Surg Res, 7(pp. 28.

[27] Ali, A. A., Cristofolini, L., Schileo, E., Hu, H., Taddei, F., Kim, R. H., Rullkoetter, P. J., and Laz, P. J., 2014, "Specimen-Specific Modeling of Hip Fracture Pattern and Repair," J Biomech, 47(2), pp. 536-43.

[28] Adouni, M., and Shirazi-Adl, A., 2014, "Evaluation of Knee Joint Muscle Forces and Tissue Stresses-Strains During Gait in Severe Oa Versus Normal Subjects," J Orthop Res, 32(1), pp. 69-78.

[29] Yao, J., Snibbe, J., Maloney, M., and Lerner, A. L., 2006, "Stresses and Strains in the Medial Meniscus of an Acl Deficient Knee under Anterior Loading: A Finite Element Analysis with Image-Based Experimental Validation," J Biomech Eng, 128(1), pp. 135-41.

[30] Papaioannou, G., Nianios, G., Mitrogiannis, C., Fyhrie, D., Tashman, S., and Yang, K. H., 2008, "Patient-Specific Knee Joint Finite Element Model Validation with High-Accuracy Kinematics from Biplane Dynamic Roentgen Stereogrammetric Analysis," J Biomech, 41(12), pp. 2633-8.

[31] Anderson, A. E., Ellis, B. J., and Weiss, J. A., 2007, "Verification, Validation and Sensitivity Studies in Computational Biomechanics," Comput Methods Biomech Biomed Engin, 10(3), pp. 171-84.

[32] Bao, H. R., Zhu, D., Gong, H., and Gu, G. S., 2013, "The Effect of Complete Radial Lateral Meniscus Posterior Root Tear on the Knee Contact Mechanics: A Finite Element Analysis," J Orthop Sci, 18(2), pp. 256-63.

[33] Perie, D., and Hobatho, M. C., 1998, "In Vivo Determination of Contact Areas and Pressure of the Femorotibial Joint Using Non-Linear Finite Element Analysis," Clin Biomech (Bristol, Avon), 13(6), pp. 394-402.

[34] Beillas, P., Lee, S. W., Tashman, S., and Yang, K. H., 2007, "Sensitivity of the Tibio-Femoral Response to Finite Element Modeling Parameters," Comput Methods Biomech Biomed Engin, 10(3), pp. 209-21.

[35] Beillas, P., Papaioannou, G., Tashman, S., and Yang, K. H., 2004, "A New Method to Investigate in Vivo Knee Behavior Using a Finite Element Model of the Lower Limb," J Biomech, 37(7), pp. 1019-30.

[36] Yang, N. H., Canavan, P. K., Nayeb-Hashemi, H., Najafi, B., and Vaziri, A., 2010, "Protocol for Constructing Subject-Specific Biomechanical Models of Knee Joint," Comput Methods Biomech Biomed Engin, 13(5), pp. 589-603.

[37] Yang, N. H., Nayeb-Hashemi, H., Canavan, P. K., and Vaziri, A., 2010, "Effect of Frontal Plane Tibiofemoral Angle on the Stress and Strain at the Knee Cartilage During the Stance Phase of Gait," J Orthop Res, 28(12), pp. 1539-47.

[38] Tranberg, R., Saari, T., Zugner, R., and Karrholm, J., 2011, "Simultaneous Measurements of Knee Motion Using an Optical Tracking System and Radiostereometric Analysis (Rsa)," Acta Orthop, 82(2), pp. 171-6.

[39] Benoit, D. L., Ramsey, D. K., Lamontagne, M., Xu, L., Wretenberg, P., and Renstrom, P., 2006, "Effect of Skin Movement Artifact on Knee Kinematics During Gait and Cutting Motions Measured in Vivo," Gait Posture, 24(2), pp. 152-64.

[40] Li, K., Zheng, L., Tashman, S., and Zhang, X., 2012, "The Inaccuracy of Surface-Measured Model-Derived Tibiofemoral Kinematics," J Biomech, 45(15), pp. 2719-23.

[41] Bourne, D. A., Choo, A. M., Regan, W. D., Macintyre, D. L., and Oxland, T. R., 2011, "The Placement of Skin Surface Markers for Non-Invasive Measurement of Scapular Kinematics Affects Accuracy and Reliability," Ann Biomed Eng, 39(2), pp. 777-85.

[42] Lindner, F., Roemer, K., and Milani, T. L., 2007, "Analysis of Skeletal Motion Kinematics for a Knee Movement Cycle," International Symposium on Biomechanics in Sports, 25(pp. 188-91.

[43] Yao, J., Salo, A. D., Lee, J., and Lerner, A. L., 2008, "Sensitivity of Tibio-Menisco-Femoral Joint Contact Behavior to Variations in Knee Kinematics," J Biomech, 41(2), pp. 390-8.

[44] Anderson, A. E., Ellis, B. J., Maas, S. A., Peters, C. L., and Weiss, J. A., 2008, "Validation of Finite Element Predictions of Cartilage Contact Pressure in the Human Hip Joint," J Biomech Eng, 130(5), pp. 051008.

[45] Walker, P. S., and Erkman, M. J., 1975, "The Role of the Menisci in Force Transmission across the Knee," Clin Orthop Relat Res, 109), pp. 184-92.

[46] Bae, J. Y., Park, K. S., Seon, J. K., Kwak, D. S., Jeon, I., and Song, E. K., 2012, "Biomechanical Analysis of the Effects of Medial Meniscectomy on Degenerative Osteoarthritis," Med Biol Eng Comput, 50(1), pp. 53-60.

[47] Guess, T. M., Thiagarajan, G., Kia, M., and Mishra, M., 2010, "A Subject Specific Multibody Model of the Knee with Menisci," Med Eng Phys, 32(5), pp. 505-15.

[48] Kurosawa, H., Fukubayashi, T., and Nakajima, H., 1980, "Load-Bearing Mode of the Knee Joint: Physical Behavior of the Knee Joint with or without Menisci," Clin Orthop Relat Res, 149), pp. 283-90.

[49] Anderst, W., Zauel, R., Bishop, J., Demps, E., and Tashman, S., 2009, "Validation of Three-Dimensional Model-Based Tibio-Femoral Tracking During Running," Med Eng Phys, 31(1), pp. 10-6.

[50] Bey, M. J., Zauel, R., Brock, S. K., and Tashman, S., 2006, "Validation of a New Model-Based Tracking Technique for Measuring Three-Dimensional, in Vivo Glenohumeral Joint Kinematics," J Biomech Eng, 128(4), pp. 604-9.

[51] Besier, T. F., Gold, G. E., Beaupre, G. S., and Delp, S. L., 2005, "A Modeling Framework to Estimate Patellofemoral Joint Cartilage Stress in Vivo," Med Sci Sports Exerc, 37(11), pp. 1924-30.

[52] Donahue, T. L., Hull, M. L., Rashid, M. M., and Jacobs, C. R., 2002, "A Finite Element Model of the Human Knee Joint for the Study of Tibio-Femoral Contact," J Biomech Eng, 124(3), pp. 273-80.

[53] Pena, E., Calvo, B., Martinez, M. A., and Doblare, M., 2006, "A Three-Dimensional Finite Element Analysis of the Combined Behavior of Ligaments and Menisci in the Healthy Human Knee Joint," J Biomech, 39(9), pp. 1686-701.

[54] Pena, E., Calvo, B., Martinez, M. A., and Doblare, M., 2008, "Computer Simulation of Damage on Distal Femoral Articular Cartilage after Meniscectomies," Comput Biol Med, 38(1), pp. 69-81.

[55] Pena, E., Calvo, B., Martinez, M. A., Palanca, D., and Doblare, M., 2006, "Why Lateral Meniscectomy Is More Dangerous Than Medial Meniscectomy. A Finite Element Study," J Orthop Res, 24(5), pp. 1001-10.

[56] Vadher, S. P., Nayeb-Hashemi, H., Canavan, P. K., and Warner, G. M., 2006, "Finite Element Modeling Following Partial Meniscectomy: Effect of Various Size of Resection," Conf Proc IEEE Eng Med Biol Soc, 1(pp. 2098-101.

[57] Zielinska, B., and Donahue, T. L., 2006, "3d Finite Element Model of Meniscectomy: Changes in Joint Contact Behavior," J Biomech Eng, 128(1), pp. 115-23.

[58] Yang, N., Nayeb-Hashemi, H., and Canavan, P. K., 2009, "The Combined Effect of Frontal Plane Tibiofemoral Knee Angle and Meniscectomy on the Cartilage Contact Stresses and Strains," Ann Biomed Eng, 37(11), pp. 2360-72.

[59] Bendjaballah, M. Z., Shirazi-Adl, A., and Zukor, D. J., 1998, "Biomechanical Response of the Passive Human Knee Joint under Anterior-Posterior Forces," Clin Biomech (Bristol, Avon), 13(8), pp. 625-633.

[60] Bendjaballah, M. Z., Shirazi-Adl, A., and Zukor, D. J., 1997, "Finite Element Analysis of Human Knee Joint in Varus-Valgus," Clin Biomech (Bristol, Avon), 12(3), pp. 139-148.

[61] Yao, J., Funkenbusch, P. D., Snibbe, J., Maloney, M., and Lerner, A. L., 2006, "Sensitivities of Medial Meniscal Motion and Deformation to Material Properties of Articular Cartilage, Meniscus and Meniscal Attachments Using Design of Experiments Methods," J Biomech Eng, 128(3), pp. 399-408.

[62] Armstrong, C. G., Lai, W. M., and Mow, V. C., 1984, "An Analysis of the Unconfined Compression of Articular Cartilage," J Biomech Eng, 106(2), pp. 165-73.

[63] Eberhardt, A. W., Keer, L. M., Lewis, J. L., and Vithoontien, V., 1990, "An Analytical Model of Joint Contact," J Biomech Eng, 112(4), pp. 407-13.

[64] Atmaca, H., Kesemenli, C. C., Memisoglu, K., Ozkan, A., and Celik, Y., 2012, "Changes in the Loading of Tibial Articular Cartilage Following Medial Meniscectomy: A Finite Element Analysis Study," Knee Surg Sports Traumatol Arthrosc, pp.

[65] Barry, M. J., Kwon, T. H., and Dhaher, Y. Y., 2010, "Probabilistic Musculoskeletal Modeling of the Knee: A Preliminary Examination of an Acl-Reconstruction," Conf Proc IEEE Eng Med Biol Soc, 2010(pp. 5440-3.

[66] Dhaher, Y. Y., Kwon, T. H., and Barry, M., 2010, "The Effect of Connective Tissue Material Uncertainties on Knee Joint Mechanics under Isolated Loading Conditions," J Biomech, 43(16), pp. 3118-25.

[67] Haut Donahue, T. L., Hull, M. L., Rashid, M. M., and Jacobs, C. R., 2003, "How the Stiffness of Meniscal Attachments and Meniscal Material Properties Affect Tibio-Femoral Contact Pressure Computed Using a Validated Finite Element Model of the Human Knee Joint," J Biomech, 36(1), pp. 19-34.

[68] Moglo, K. E., and Shirazi-Adl, A., 2005, "Cruciate Coupling and Screw-Home Mechanism in Passive Knee Joint During Extension--Flexion," J Biomech, 38(5), pp. 1075-83.

[69] Li, G., Lopez, O., and Rubash, H., 2001, "Variability of a Three-Dimensional Finite Element Model Constructed Using Magnetic Resonance Images of a Knee for Joint Contact Stress Analysis," J Biomech Eng, 123(4), pp. 341-6.

[70] Pena, E., Calvo, B., Martinez, M. A., Palanca, D., and Doblare, M., 2005, "Finite Element Analysis of the Effect of Meniscal Tears and Meniscectomies on Human Knee Biomechanics," Clin Biomech (Bristol, Avon), 20(5), pp. 498-507.

[71] Abraham, A. C., Moyer, J. T., Villegas, D. F., Odegard, G. M., and Haut Donahue, T. L., 2011, "Hyperelastic Properties of Human Meniscal Attachments," J Biomech, 44(3), pp. 413-8.

[72] Mononen, M. E., Jurvelin, J. S., and Korhonen, R. K., 2013, "Effects of Radial Tears and Partial Meniscectomy of Lateral Meniscus on the Knee Joint Mechanics During the Stance Phase of the Gait Cycle-a 3d Finite Element Study," J Orthop Res, 31(8), pp. 1208-17.

[73] Donzelli, P. S., Spilker, R. L., Ateshian, G. A., and Mow, V. C., 1999, "Contact Analysis of Biphasic Transversely Isotropic Cartilage Layers and Correlations with Tissue Failure," J Biomech, 32(10), pp. 1037-47.

[74] Shepherd, D. E., and Seedhom, B. B., 1999, "The 'Instantaneous' Compressive Modulus of Human Articular Cartilage in Joints of the Lower Limb," Rheumatology (Oxford), 38(2), pp. 124-32.

[75] Haemer, J. M., Song, Y., Carter, D. R., and Giori, N. J., 2011, "Changes in Articular Cartilage Mechanics with Meniscectomy: A Novel Image-Based Modeling Approach and Comparison to Patterns of Oa," J Biomech, 44(12), pp. 2307-12.

[76] Hosseini, A., Van De Velde, S., Gill, T. J., and Li, G., 2012, "Tibiofemoral Cartilage Contact Biomechanics in Patients after Reconstruction of a Ruptured Anterior Cruciate Ligament," J Orthop Res, 30(11), pp. 1781-8.

[77] Shefelbine, S. J., Ma, C. B., Lee, K. Y., Schrumpf, M. A., Patel, P., Safran, M. R., Slavinsky, J. P., and Majumdar, S., 2006, "Mri Analysis of in Vivo Meniscal and Tibiofemoral Kinematics in Acl-Deficient and Normal Knees," J Orthop Res, 24(6), pp. 1208-17.

[78] Bingham, J. T., Papannagari, R., Van De Velde, S. K., Gross, C., Gill, T. J., Felson, D. T., Rubash, H. E., and Li, G., 2008, "In Vivo Cartilage Contact Deformation in the Healthy Human Tibiofemoral Joint," Rheumatology (Oxford), 47(11), pp. 1622-7.

[79] Li, G., Defrate, L. E., Park, S. E., Gill, T. J., and Rubash, H. E., 2005, "In Vivo Articular Cartilage Contact Kinematics of the Knee: An Investigation Using Dual-Orthogonal Fluoroscopy and Magnetic Resonance Image-Based Computer Models," Am J Sports Med, 33(1), pp. 102-7.

[80] Van De Velde, S. K., Bingham, J. T., Hosseini, A., Kozanek, M., Defrate, L. E., Gill, T. J., and Li, G., 2009, "Increased Tibiofemoral Cartilage Contact Deformation in Patients with Anterior Cruciate Ligament Deficiency," Arthritis Rheum, 60(12), pp. 3693-702.

[81] Von Eisenhart-Rothe, R., Lenze, U., Hinterwimmer, S., Pohlig, F., Graichen, H., Stein, T., Welsch, F., and Burgkart, R., 2012, "Tibiofemoral and Patellofemoral Joint 3d-Kinematics in Patients with Posterior Cruciate Ligament Deficiency Compared to Healthy Volunteers," BMC Musculoskelet Disord, 13(1), pp. 231-238.

[82] Woo, S. L., Debski, R. E., Withrow, J. D., and Janaushek, M. A., 1999, "Biomechanics of Knee Ligaments," Am J Sports Med, 27(4), pp. 533-43.

[83] Delp, S. L., Anderson, F. C., Arnold, A. S., Loan, P., Habib, A., John, C. T., Guendelman, E., and Thelen, D. G., 2007, "Opensim: Open-Source Software to Create and Analyze Dynamic Simulations of Movement," IEEE Trans Biomed Eng, 54(11), pp. 1940-50.

[84] Netravali, N. A., Koo, S., Giori, N. J., and Andriacchi, T. P., 2011, "The Effect of Kinematic and Kinetic Changes on Meniscal Strains During Gait," J Biomech Eng, 133(1), pp. 011006.

[85] Abraham, A. C., Villegas, D. F., Kaufman, K. R., and Haut Donahue, T. L., 2013, "Internal Pressure of Human Meniscal Root Attachments During Loading," J Orthop Res, 31(10), pp. 1507-13.

[86] Dong, Y., Hu, G., Dong, Y., Hu, Y., and Xu, Q., 2013, "The Effect of Meniscal Tears and Resultant Partial Meniscectomies on the Knee Contact Stresses: A Finite Element Analysis," Comput Methods Biomech Biomed Engin, pp.

[87] Mononen, M. E., Jurvelin, J. S., and Korhonen, R. K., 2013, "Implementation of a Gait Cycle Loading into Healthy and Meniscectomised Knee Joint Models with Fibril-Reinforced Articular Cartilage," Comput Methods Biomech Biomed Engin, pp.

[88] Carey, R. E., Zheng, L., Aiyangar, A. K., Harner, C. D., and Zhang, X., In press, "Subject-Specific Finite Element Modeling of the Tibiofemoral Joint Based on Ct, Magnetic Resonance Imaging and Dynamic Stereo-Radiography Data in Vivo," J Biomech Eng, In press(In press), pp. In press.

[89] Segal, N. A., Anderson, D. D., Iyer, K. S., Baker, J., Torner, J. C., Lynch, J. A., Felson, D. T., Lewis, C. E., and Brown, T. D., 2009, "Baseline Articular Contact Stress Levels Predict Incident Symptomatic Knee Osteoarthritis Development in the Most Cohort," J Orthop Res, 27(12), pp. 1562-8.

[90] Kuster, M., Wood, G. A., Sakurai, S., and Blatter, G., 1994, "1994 Nicola Cerulli Young Researchers Award. Downhill Walking: A Stressful Task for the Anterior Cruciate

Ligament? A Biomechanical Study with Clinical Implications," Knee Surg Sports Traumatol Arthrosc, 2(1), pp. 2-7.

[91] Li, G., Gil, J., Kanamori, A., and Woo, S. L., 1999, "A Validated Three-Dimensional Computational Model of a Human Knee Joint," J Biomech Eng, 121(6), pp. 657-62.

[92] Arnold, E. M., Ward, S. R., Lieber, R. L., and Delp, S. L., 2010, "A Model of the Lower Limb for Analysis of Human Movement," Ann Biomed Eng, 38(2), pp. 269-79.

[93] Steele, K. M., Demers, M. S., Schwartz, M. H., and Delp, S. L., 2012, "Compressive Tibiofemoral Force During Crouch Gait," Gait Posture, 35(4), pp. 556-60.

[94] Zheng, L., Aiyangar, A. K., Carey, R. E., Lippert, C., Harner, C. D., and Zhang, X., 2012, "Patient-Specific Musculoskeletal Modeling for Evaluating the Efficacy of Meniscus Transplantation," eds., University of Florida, Gainesville, Florida, USA, pp.

[95] Lynn, S. K., Reid, S. M., and Costigan, P. A., 2007, "The Influence of Gait Pattern on Signs of Knee Osteoarthritis in Older Adults over a 5-11 Year Follow-up Period: A Case Study Analysis," Knee, 14(1), pp. 22-8.